



Experimental characterization of hybrid structural components  
(Concrete reinforced by profiles)

Submitted By

**Md. Refat Ahmed Bhuiyan**

Under the supervision of

**Prof. Dr. Hervé Degée**

European Erasmus Mundus Master Course  
Sustainable Constructions  
Under Natural Hazards and Catastrophic Events  
520121-1-2011-1-CZ-ERA MUNDUS-EMMC

## **ACKNOWLEDGEMENT**

First of all, I offer my sincerest gratitude to my supervisor, Dr Herve Degee, who has supported me throughout my thesis with his patience and knowledge whilst allowing me the room to work in my own way. I attribute the level of my Master's degree to his encouragement and effort and without him this thesis, too, would not have been completed or written. One simply could not wish for a better or friendlier supervisor.

This project paper is completed with the cordial supervision of the project supervisor Dr. Herve Degee, Professor of civil engineering department, ULg.

Authors also express their intense gratitude and appreciation to Dr. Boyan Mihaylov and Dr. Teodora Bogdan for their proper guidance, cordial co-operation and supervision throughout the period of project completion.

I would also like to thank Structural Engineering Department, University of Liege. And finally, for the financial support I would like to thank European Commission, without their financial contribution it would not be possible to complete.

December, 2013

ULg

## **ABSTRACT**

The structural system referred to as the steel-concrete hybrid structure is frequently adopted in many countries for the construction of buildings and bridges, even in the regions of high seismic risk. These hybrid elements rely on the transfer of force between the two materials in order to realize the benefits of hybrid action. And the problems in design are related to the problem of force transmission between concrete and embedded steel profiles, a situation in which it is not known how to combine the resistances provided by bond, by stud connectors and by plate bearings, and how to reinforced the concrete in the transition zone.

This report covers the theoretical design and numerical modeling of some hybrid specimen to transfer of forces from the steel profile to the concrete wall without creating local disturbances.

This study gives a clear idea about the load transfer mechanism between various types of connectors. Rigid connectors like plate bearing are better than flexible connectors because of their struts and tie effects. Area of the concrete section where load is transferred and the concrete grade is also directly related with the shear resistance capacity. Finally this study gives some idea about the shear resistance of composite section and future work but the real behavior and load transfer mechanism can be achieved by physical experiment.

# **INDEX SHEET**

## **CHAPTER 01: INTRODUCTION**

1.1	General	11
1.2	Objective	12

## **CHAPTER 02: REVIEW OF LITERATURE**

2.1	Definition of work	13
2.2	General rules in Euro code 4	13
2.2.1	Resistance to shear	14
2.2.2	Bond-Slip Relationship	15
2.2.3	Shear bond stress-slip behavior	16
2.2.4	Profile concrete bond stress	16
2.3	Headed stud shear connector	16
2.3.1	Load bearing behavior	17
2.3.2	Stud shear mechanism	17
2.3.3	Effect of various parameters	18
2.3.4	Bearing capacity	18
2.3.5	Load-slip relationship	19
2.4	Compression struts bearing	19
2.4.1	What is strut-and-tie model	19
2.4.2	Strut and tie model components	20
2.4.3	Design stress for compression struts	21

2.4.4 Strut and tie design in Eurocode	21
--	----

## **CHAPTER 03: RESEARCH METHODOLOGY**

3.1 Materials	22
3.1.1 Concrete	22
3.1.2 Steel profile	23
3.1.3 Reinforcement	23
3.2 Specimen details	23
3.2.1 Concrete wall	23
3.2.2 Embedded steel profile	24
3.2.3 Configuration A and C	24
3.2.4 Configuration B and D	25
3.2.5 Configuration E	25
3.3 FEM software	26

## **CHAPTER FOUR: DESIGN AND NUMERICAL MODELING**

4.1 Theoretical design	27
4.1.1 Configuration A and C	27
4.1.2 Configuration B and D	28
4.1.3 Configuration E	31
4.1.4 Summary	31

4.2 Numerical modeling of the specimens	33
4.2.1 Configuration A and C	33
4.2.2 Configuration B and D	35
4.2.2.1 Model01	35
4.2.2.2 Model02	36
4.2.3 Configuration E	37

## **CHAPTER FIVE: RESULT AND INTERPRETATION**

5.1 Configuration A and C	39
5.1.1 Configuration A (SP1A)	39
5.1.2 Configuration C (SP2C)	41
5.1.3 Summary	42
5.2 Configuration B and D	43
5.2.1 Model01	43
5.2.2 Model02	45
5.2.3 Summary	49
5.3 Configuration E	50
5.4 Effect of concrete grade	52

## **CHAPTER FIVE: RESULT AND INTERPRETATION**

6.1 Summary and conclusion	53
6.2 Suggestion for future work	54

## INDEX OF FIGURE AND TABLE

No	Name	Page
01	Figure 1.1: Specimen configuration	12
02	Figure 2.2.1: Typical shear resistance versus slip behavior	14
03	Figure 2.2.2: Analytical Bond-stress slip relationship	15
04	Figure 2.3.1: Load transfer of a headed stud connector in a solid slab	17
05	Figure 2.4.1: Examples of Strut-and-Tie Models	20
06	Figure 2.4.2: Basic Type of Struts in a 2-D Members	20
07	Figure 2.4.3: Type of Nodes	20
08	Figure 2.4.4: Figure C2(e) of EN1998-1-1.	21
09	Figure 3.1.1: Popovics pre- and post-peak concrete compression responses	22
10	Figure 3.1.2: Bi-linear stress-strain relationship	23
11	Figure 3.2.3: Configuration A and C	25
12	Figure 3.2.4: Configuration B and D.	25
13	Figure 3.2.5: Configuration E	25
14	Figure 4.1.2: Strut & tie model to determine plate connector strength.	28
15	Figure 4.1.3. Internal bearing plate yield line pattern (fixed condition)	29
16	Figure 4.1.4. Weld dimensions of the plate connector.	30
17	Table 4.1.4: Summary of design resistances of specimens	32
18	Figure 4.2.1a: Shear studs modeling	33
19	Figure 4.2.1b: Load-slip relationship for shear studs	34
20	Table 4.2.1: Details of Specimen SP1A and SP2C	35
21	Figure 4.2.2.1: Modeling of specimen SPBM1 and SPDM1	36

22	Table 4.2.2.2: Specimen details of SPBM2 and SPDM2	37
23	Table 4.2.3: Specimen details of SPEM2	38
24	Figure 5.1.1 (a-g) results SP1A	39
25	Figure 5.1.2 (a-g) results SP1C	41
26	Table 5.2.1: FEM analysis result for SPBM1 and SPDM1	43
27	Figure 5.1.2 (a-h) results for SPBM1 and SPDM1	44
28	Table 5.2.2a: FEM analysis result for SPBM2	46
29	Figure 5.2.2 (a-f) results for SPBM2	46
30	Table 5.2.2b: FEM analysis result for SPDM2	48
31	Figure 5.2.2 (g-l) results for SPDM2	48
32	Table 5.3: FEM analysis result for SPEM2	50
33	Figure 5.3: (a-d) results for SPEM2	51
34	Table 5.4 Effect of concrete grade	52

## **BIBLIOGRAPHY**

## **ANNEX**



## UNITS AND NOTATIONS

$E_s$  = Modulus of elasticity of the steel

$d_b$  = Bar diameter

$d_v$  = Effective shear depth

$f_c'$  = Concrete cylinder strength

$f_{c1}$  = Average principal tensile stress in cracked concrete

$f_{ce}$  = Effective concrete strength in models of the Theory of Plasticity

$f_{ck}$  = Characteristic concrete cylinder strength according to EC2

$f_y$  = Yield strength of flexural reinforcement

$f_{c2}$  = Average principal compressive stress in cracked concrete

$\epsilon$  = Strain

$\epsilon_{sh}$  = reinforcement strain at onset of strain hardening

$\epsilon_t$  = Average strain in the bottom longitudinal reinforcement over the shear span

$\mu$  = Poisson's ratio

$f_s$  = characteristic strength of steel

$\rho$  = reinforcement ratio

$P_U$  = bearing capacity of stud

$E_c$  = elastic modulus of concrete

$\gamma_v$  = partial safety factor

$F_{Rd}$  = design value of force in strut and tie model

$E_a$  = steel modulus of elasticity

$N_{pIRd}$ = plastic resistance of steel profile

$P_{Rk}$ = shear stud connector strength

kN= kilo newton

MPa= mega Pascal

$A_{sv}$ = area of vertical reinforcement

$A_{sh}$ = area of horizontal reinforcement

$\sigma$  = axial stress

## CHAPTER: ONE

### INTRODUCTION

#### **1.1 General:**

The structural system referred to as the steel-concrete hybrid structure is frequently adopted in many countries for the construction of buildings and bridges, even in the regions of high seismic risk. Steel concrete hybrid structure is composed of the composite structure and the mixed structure. Hybrid steel and concrete elements can take many forms. Examples include the steel girder with concrete slab, concrete pier with steel girder, steel framing of a building with the concrete floor slabs, the encasement of a steel element with concrete, or the filling of a steel hollow section with concrete. These hybrid elements rely on the transfer of force between the two materials in order to realize the benefits of hybrid action.

Benefits can include an increase in strength and stiffness as well as the restraint of buckling instabilities in the steel or confinement of the concrete. Hybrid action can be achieved through mechanical connection between the steel and concrete members or elements. The problem with those hybrid structures is that they are neither reinforced concrete structure in the sense of Eurocode 2 or ACI318, nor composite steel concrete structure in the sense of Eurocode 4 or ASCE10. The problems with hybrid element design are mostly related to the problem of force transmission between concrete and embedded steel profiles, a situation in which it is not known how to combine the resistances provided by bond, by stud connectors and by plate bearings, and how to reinforced the concrete in the transition zone.

To investigate the complicated behavior of the hybrid structures or its components, the experimental investigation is the key resource. Besides the experimental investigation, numerical evaluation also plays a significant role to examine the structural behavior and mechanical properties of hybrid structures. To conduct experiment with varying geometric properties is a time consuming matter, whereas numerical analysis can easily check the effect of any variation. In this case my study involves numerical analysis of some hybrid structural component.

## 1.2 Objectives:

The aim of the thesis is to design and numerical analysis of composite structural elements to study the transfer mechanism of compression or tension forces from the steel to the concrete. It includes theoretical design with existing codes and numerical modeling of some composite specimens. The study mainly involve with the investigation of the load transfer from the steel profile to the concrete wall without creating local disturbances, like transverse cracking or splitting of concrete around the steel profile. In this case we consider some reinforced concrete specimen with embedded steel profile. The failure load should be less than the concrete and steel profile capacity to confirm the failure occurs in the connection between steel and concrete. In this study two types of connection is used, one is stud connector and another is plate bearing. To achieve the goal of this thesis, this study has been done with some similar specimen with different configuration of shear connectors, plate bearings.

5 tests specimens are taken into consideration as described below: (Figure: 1.1)

- A. steel profile strong axis perpendicular to wall face; long connection with flexible connectors on total length of the steel encased profile; no end plate; polystyrene at the end of the steel profile; transverse links at each connector (Configuration-A)
- B. steel profile strong axis perpendicular to wall face; short connection with stiff connectors (transverse stiffener type); no end plate; polystyrene at the end of the steel profile; transverse links as from strut and ties design (Configuration-B)
- C. steel profile weak axis perpendicular to wall face; long connection with flexible connectors on total length of the steel encased profile; no end plate; polystyrene at the end of the steel profile; transverse links at each connector (Configuration-C)
- D. steel profile weak axis perpendicular to wall face; short connection with stiff connectors (transverse stiffener type); no end plate; polystyrene at the end of the steel profile; transverse links as from strut and ties design (Configuration-D)
- E. steel profile weak axis perpendicular to wall face; combined long and short connection with flexible and stiff connectors on total length of the steel encased profile; no end plate; polystyrene at the end of the steel profile; transverse links at each connector (Configuration-E)

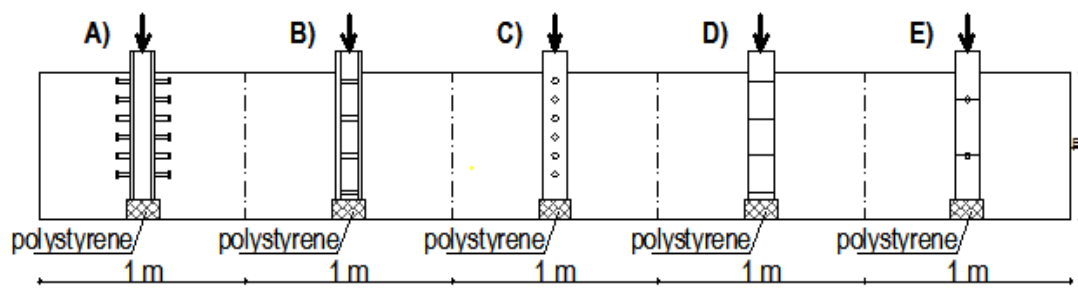


Figure 1.1 specimen configuration

## CHAPTER: TWO

### REVIEW OF LITERATURE

#### 2.1 Definition of work

“Identification of the fundamental force transfer mechanisms at steel-concrete interface”

In this case a preliminary study of the force transfer mechanisms based on an extensive review of the existing literature. The objective is to identify those mechanisms and to organize the existing data and methods, if any, in a ready to use form. The references considered are Eurocode 2: EN1992-1-1:2004 and Eurocode 4: EN1994-1-1:2004.

#### 2.2 General rules in Eurocode 4

EC4-6.7.4.1 (1)P Provision shall be made in regions of load introduction for internal forces and moments applied from members connected to the ends and for loads applied within the length to be distributed between the steel and concrete components, considering the shear resistance at the interface between steel and concrete. A clearly defined load path shall be provided that does not involve an amount of slip at this interface that would invalidate the assumptions made in design.

EC4-6.7.4.1 (2)P Where composite columns and compression members are subjected to significant transverse shear, as for example by local transverse loads and by end moments, provision shall be made for the transfer of the corresponding longitudinal shear stress at the interface between steel and concrete.

EC4-6.7.4.1 (3) For axially loaded columns and compression members, longitudinal shear outside the areas of load introduction need not be considered.

EC4-6.7.4.2 (1) Shear connectors should be provided in the load introduction area and in areas with change of cross section, if the design shear strength  $\tau_{Rd}$ , see 6.7.4.3, is exceeded at the interface between steel and concrete. The shear forces should be determined from the change of sectional forces of the steel or reinforced concrete section within the introduction length. If the loads are introduced into the concrete cross section only, the values resulting from an elastic analysis considering creep and shrinkage should be taken into account. Otherwise, the forces at the interface should be determined by elastic theory or plastic theory, to determine the more severe case.

EC4-6.7.4.2 (2) In absence of a more accurate method, the introduction length should not exceed  $2d$  or  $L/3$ , where  $d$  is the minimum transverse dimension of the column and  $L$  is the column length.

EC4-6.7.4.2 (3) For composite columns and compression members no shear connection need be provided for load introduction by endplates if the full interface between the concrete

section and endplate is permanently in compression, taking account of creep and shrinkage. Otherwise the load introduction should be verified according to (5). For concrete filled tubes of circular cross-section the effect caused by the confinement may be taken into account if the conditions given in 6.7.3.2(6) are satisfied using the values  $\eta_a$  and  $\eta_c$  for  $\bar{\lambda}$  equal to zero.

EC4-6.7.4.2 (4) Where stud connectors are attached to the web of a fully or partially concrete encased steel I-section or a similar section, account may be taken of the frictional forces that develop from the prevention of lateral expansion of the concrete by the adjacent steel flanges. This resistance may be added to the calculated resistance of the shear connectors. The additional resistance may be assumed to be  $\mu PRd$  on each flange and each horizontal row of studs, where  $\mu$  is the relevant coefficient of friction that may be assumed. For steel sections without painting,  $\mu$  may be taken as 0,5.  $PRd$  is the resistance of a single stud in accordance with 6.6.3.1. In absence of better information from tests, the clear distance between the flanges should not exceed the values.

### 2.2.1 Resistance to shear

The shear force transfer at the connection between concrete and steel components is typically carried by three main mechanisms: a) chemical bonding (bond between the cement paste and the surface of the steel: b) friction (assumed proportional to the normal force at the interface): c) mechanical interaction (due to embossments, ribs or shear stud connectors). While chemical bonding is typically neglected in both design and analysis of composite structures, friction and especially mechanical actions are very important (Salari (1999)).

It is common practice to design composite slabs as one way slabs with slab action parallel to the ribs. Shear connectors between concrete slab and steel section are considered to provide the required composite action in flexure. They can also be used to distribute the large horizontal inertial forces in the slab to the main lateral load resisting elements of the structure (Hawkins and Mitchell (1984)). Headed shear connectors are welded to the steel beam to provide different degrees of connection between the concrete slab and beam.

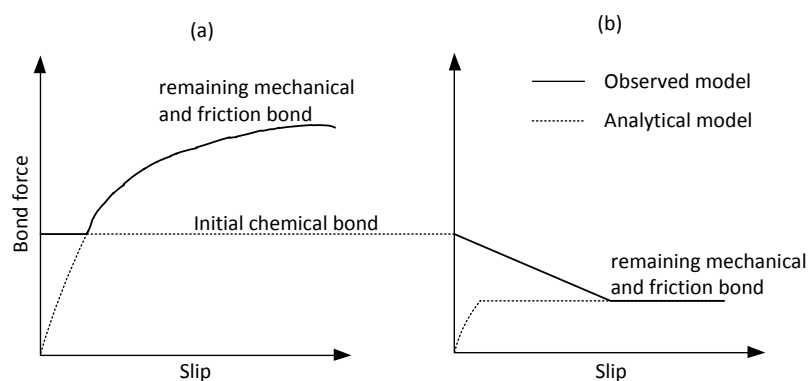


Figure 2.2.1: Typical shear resistance versus slip behavior:  
a) ductile response; b) brittle response

The shear force transfer in composite members is experimentally measured using different techniques. The push-out test is the most common procedure because of its simplicity. Figure 2.2.1 shows a qualitative shear resistance versus slip behavior (Daniels and Crisinel (1993, Daniels and Crisinel (1993))). Two different behaviors labeled "ductile" and "brittle" are distinguished. Brittle behavior is observed (case b). Brittle failures are typically associated with decking with small or no embossments, and without shear studs. In embossed decks or when shear studs are added, the bond stresses associated with these mechanical devices are much higher than the chemical bond stresses and the response is ductile (case a). In both cases the initial chemical bond associated with no slip is neglected in design and analysis, as shown in Figure 2.2.1 by the dotted line.

### 2.2.2 Local bond – slip relationship

Under well-defined conditions, it is possible to consider that there is an average 'Local bond' versus 'Local slip' relationship, for short anchorage lengths, statistically acceptable, see Figure 2.2.2.

The bond stress-slip relationship depends on a considerable number of influencing factors like rib geometry (related rib area), concrete strength, position and orientation of the bar during casting, state of stress, boundary conditions and concrete cover. Therefore the bond stress-slip curves for confined and unconfined concrete, presented in Figure 2.2.2, can be considered as statistical mean curves, applicable as an average formulation for a broad range of cases

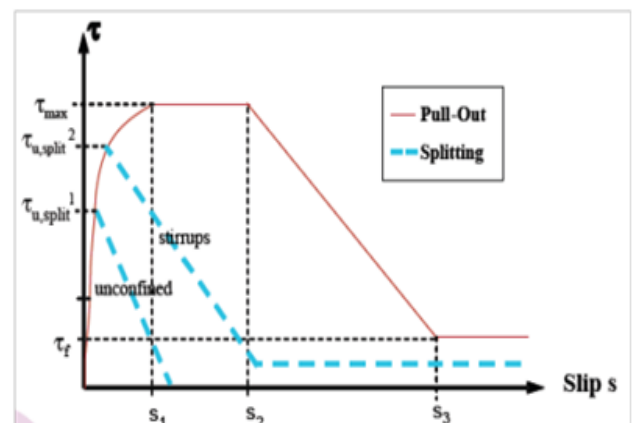


Figure 2.2.2: Analytical Bond-stress slip relationship

The first curved part refers to the stage in which the ribs penetrate into the mortar matrix, characterized by local crushing and micro-cracking. The horizontal level occurs only for confined concrete. The decreasing branch refers to the reduction of bond resistance due to shearing of the concrete corbels between the ribs. In case of unconfined concrete splitting failure occurs which is reflected by a sudden drop of the bond strength before the horizontal level is reached.

The parameters of the bond stress-slip relationship are first defined following the good or poor bond conditions, the presence of stirrups for the confinement, and the strain in the rebar. The split shear stress depends on the resistance of the concrete, the diameter of the bar, the concrete cover, and again the density of confining bars.

### **2.2.3 Shear bond stress- slip behaviour**

The failure behaviour of the plate is dictated by the integrity of the plate with the original concrete member through adhesive bonding, which plays the role of a shear connector between the plate and the original RC member. However, these bonded plates are prone to many failure mechanisms as categorized by Oehlers (2001). Therefore, an important issue in the design of effective retrofitting solution using externally bonded plates is the bond strength. The paper is concerned with the bond strength and the critical bond length, which is defined as the length of the externally bonded plate, beyond which there is no further increase in the axial load carrying capacity of the plate–adhesive–concrete interface. To understand the failure/debonding mechanism of the plates, complete knowledge of the bond behaviour of the plate–adhesive–concrete interface is a prerequisite (Ali et al. (2001)).

### **2.2.4 Profile-Concrete bond stress**

Many studies (Bryson and Mathey (1962); Hawkins (1973); Roeder (1984); Hamdan and Hunaiti (1991); Wium and Lebet (1991, Wium and Lebet (1992)) have addressed the bond stress capacity of SRC composite columns with push-out tests. The bond stress capacity is commonly evaluated as the maximum average bond stress, which is the maximum load transferred between the steel and concrete, divided by the total surface area of steel section embedded within the concrete. Other studies have employed the short column test, where the load is applied to the exposed steel at the top of the column but where the reaction is provided to both the concrete and steel at the base of the specimen.

For natural bond condition, their experimental results indicated that the bond stress can be determined by using the following equation (In this equation, the maximum average bond was reduced by 2 standard deviations providing an estimated confidence of 97.7%):

$$f_{s(2\sigma)} = 2.52 - 0.39 \frac{L}{d} - 19.12\rho \text{ (in MPa)}$$

where  $L$  and  $d$  are the length and depth of the steel section;  $\rho = A_s/A_t$ ;  $A_s$  and  $A_t$  are the areas of the steel section to the total cross section of the composite member.

## **2.3 Headed stud shear connectors**

Headed shear studs are by far the most common type of shear connector used in the design of composite members in steel frame construction today. Indeed this has been the case for the last 60 years. The shear stud is one of the fundamental components of any composite member in which it is used. It can therefore be argued that a thorough understanding of the performance characteristics of the shear studs is essential if efficient, reliable design of



composite members is to take place. Push-out tests are commonly used to determine the capacity of the shear connection and load-slip behavior of the shear connectors.

### 2.3.1 Load-bearing behavior

One of the most illustrated models to explain the load transfer of stud connectors in solid slab applications is given by Lungershausen (1988) where four different components which contribute to the total capacity of the connector are defined (Figure 2.3.1). Initially, the majority of the longitudinal shear force is transferred at the base of the stud into the surrounding concrete (A) where a significant amount of it reacts directly at the weld collar. The multi-axial high bearing stresses in the concrete eventually lead to local crushing failure of the concrete at the bottom of the stud and to a redistribution of the shear forces in areas higher up the shank of the stud (B). Since the top of the stud is embedded in undamaged concrete and cannot deform while the base of the connector is free to move laterally, bending and tensile stresses are induced into the shank of the stud (C). To balance these tensile stresses, compressive forces develop in the concrete under the head of the stud and are thought to activate additional frictional forces (D) at the steel concrete interface. Eventually the shear connection fails when the shank of the stud experiences a combined shear-tension failure right above the weld collar.

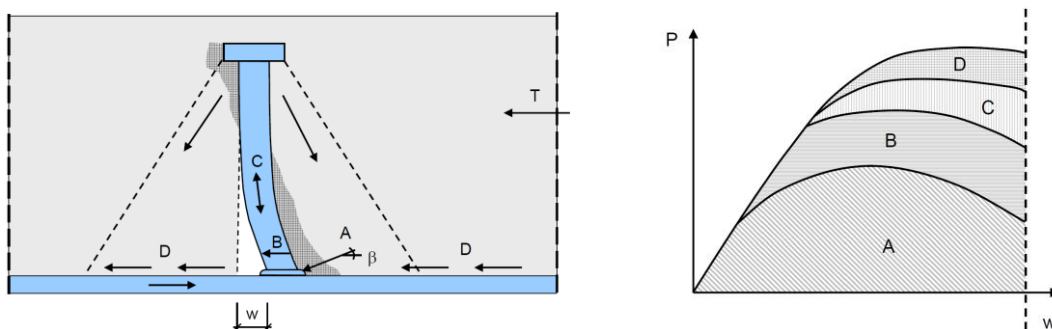


Figure 2.3.1: Load transfer of a headed stud connector in a solid slab in accordance with Lungershausen (1988).

### 2.3.2 Stud Shear Mechanism

As can be presented in Xue et al. (2008), the stud is subjected to bending moment, axial force, and shear force at the same time when the load is applied to the specimens. It can be seen that the stud shank became stretched and flat at the root part. The concrete around the stud in compression is supposed to be an ideal elastic-plastic material. The stud is subjected to the load transferred from the steel beam and the counterforce of concrete as a beam on the elastic foundation. Once the slip between the steel beam and the concrete slab occurs, concrete around end of the stud in compression starts to become deformed and the stud will rotate. At the same time, the rotation of the stud will be restricted by the concrete around

other end of the stud. The load transferred by the steel beam to the stud will increase continuously with the increase of the load imposed on the specimen.

### **2.3.3 Effects of various parameters on the stud load-slip behavior**

- Effect of stud diameter and height
- Effect of concrete strength
- Effect of stud welding technique
- Effect of transverse reinforcement
- Effect of steel beam type
- Effect of transverse arrangement

### **2.3.4 Bearing Capacity**

As mentioned by Xue et al. (2008) the calculation formula for the stud shear bearing capacity was derived based on the earlier work of Viest (1956), and the expression is

$$P_u = \begin{cases} 332d^2\sqrt{f'_c} & (H/d \geq 4.2) \\ 79Hd\sqrt{f'_c} & (H/d \leq 4.2) \end{cases}$$

where  $P_u$  = stud shear bearing capacity (k);  $d$  = stud diameter (in.);  $H$  = stud height (in.); and  $f'_c$  = compressive strength of concrete cylinders (psi).

Eurocode EC4 (2004) specified the design strength of stud shear connectors which are welded automatically, as

$$P_u = \min \left\{ \begin{array}{l} \frac{0.8f_u\pi d^2/4}{\gamma_v} \\ \frac{0.29\alpha d^2\sqrt{f_{ck}E_{cm}}}{\gamma_v} \end{array} \right\}$$

where the units are N, mm;  $d$  = diameter of the studs;  $f_u$  = ultimate tensile strength of stud;  $f_c$  = compressive strength of concrete cylinders;  $E_c$  = elastic modulus of concrete;  $\gamma_v$  = partial safety factor (=1.25);  $\alpha = 0.2(H/d+1) \leq 1$ ; and  $H$  = height of the studs.

In AISC (2005), the nominal strength of one stud shear connector embedded in solid concrete or in a composite slab is

$$P_u = 0.5A_s \sqrt{f'_c E_c} \leq R_g R_p A_s F_u$$

where  $F_u$  = specified minimum tensile strength of a stud shear connector (MPa);  $E_c$  = modulus of elasticity of concrete (MPa);  $f'_c$  = compressive strength of concrete cylinders (MPa);  $R_g = 1.0$  for any number of studs welded in a row directly to the steel shape; and  $R_p = 1.0$  for studs welded directly to the steel shape and having a haunch detail with not more than 50% of the top flange covered by a deck of sheet steel closures.

### **2.3.5 Load slip relationship:**

Mohammad Makki Abbass (2011) in his paper (ISSN 0974-5904, Volume 04, No 06 SPL) proposed a load slip relationship. After an extensive study on stud behavior he found, the slip ( $u$ ) is considered as non-dimensional parameter as a ratio of slip( $u$ ) to stud diameter( $d$ ). And here  $Q$  is the load in kN and  $f_{cu}$  is the characteristic strength of concrete.

$$Q=0.0407*(f_{cu})^{0.57}*d^2*((u/d)/(0.01245+(u/d)))$$

## **2.4 Compression Struts Bearing**

In selecting the appropriate design approach for structural concrete, it is useful to classify portions of the structure as either B- (Beam or Bernoulli) Regions or D- (Disturbed or Discontinuity) Regions. B-Regions are parts of a structure in which Bernoulli's hypothesis of straight-line strain profiles applies. D-Regions, on the other hand, are parts of a structure with a complex variation in strain. D-Regions include portions near abrupt changes in geometry (geometrical discontinuities) or concentrated forces (statical discontinuities). The main concept behind these is called strut and tie method. The idea of the strut-and-tie method came from the truss analogy method introduced independently by Ritter and Mörch in the early 1900s for shear design of B-Regions. This method employs the so-called truss model as its design basis. The model was used to idealize the flow of force in a cracked concrete beam.

### **2.4.1 What is Strut and tie models**

The STM is based on the lower-bound theory of limit analysis. In the STM, the complex flow of internal forces in the D-Region under consideration is idealized as a truss carrying the imposed loading through the region to its supports. This truss is called *strut-and-tie model* and is a statically admissible stress field in lower-bound (static) solutions. Like a real truss, a strut-and-tie model consists of *struts* and *ties* interconnected at *nodes* (also referred to as *nodal zones* or *nodal regions*). A selection of strut-and-tie models for a few typical 2-D D-Regions is illustrated in Figure 2.4.1 As shown in the figure, struts are usually symbolized using broken lines, and ties are usually denoted using solid lines.

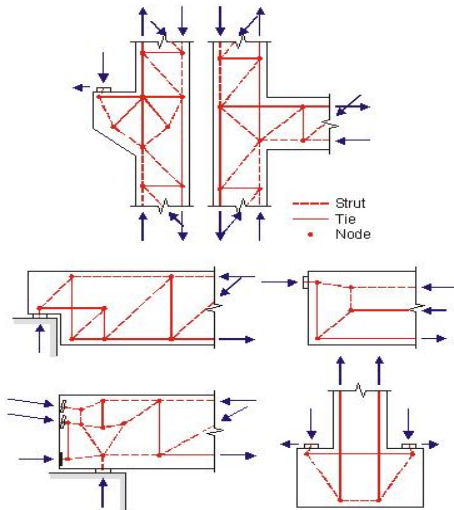


Figure 2.4.1: Examples of Strut-and-Tie Models

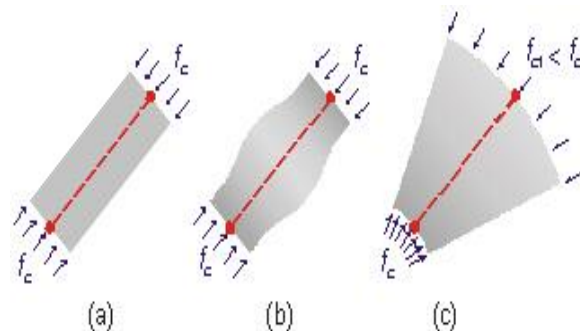


Figure 2.4.2: Basic Type of Struts in a 2-D Member

### 2.4.2 Strut-and-Tie Model Components

Struts are the compression members of a strut-and-tie model and represent concrete stress fields whose principal compressive stresses are predominantly along the centerline of the strut. The idealized shape of concrete stress field surrounding a strut in a plane (2-D) member, however, can be prismatic (Figure 2.4.2(a)), bottle-shaped (Figure 2.4.2(b)), or fan-shaped (Figure 2.4.2(c)) (Schlaich,1991). Struts can be strengthened by steel reinforcement, and if so, they are termed reinforced struts.

Ties are the tension members of a strut-and-tie model. Ties mostly represent reinforcing steel, but they can occasionally represent pre-stressing steel or concrete stress fields with principal tension predominant in the tie direction.

Nodes are analogous to joints in a truss and are where forces are transferred between struts and ties. As a result, these regions are subject to a multidirectional state of stress. Nodes are classified by the types of forces being connected. Figure 2.4.3 shows basic types of nodes in a 2-D member; in the figure,  $C$  is used to denote compression and  $T$  is used to denote tension. The stress state in concrete at nodes is different in those different basic types, which results in different design stresses for compression struts in the different types.

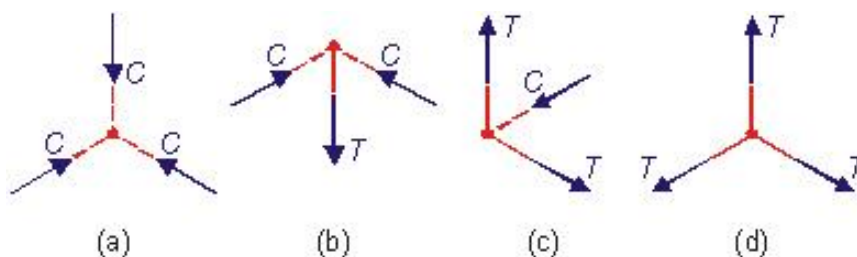


Figure 2.4.3: Type of Nodes: (a) CCC (b) CCT (c) CTT (d) TTT

### 2.4.3 Design stresses for compression struts

The design rules in Eurocode 2 or in *fib* manuals reflect the influence of the stress state by providing design values which are different for different stress states corresponding to CCC nodes, CCT nodes and CTT nodes, where C stands for compression and T stands for tension. The rules also reflect a care for safety in limiting the design stress in compression struts to  $f_{cd}$  or less in most practical cases.

Hereunder, the rules in Eurocode 2 (EN1992-1-1:2004) and in *fib* 2010 manuals on structural concrete are presented in parallel, in order to set forward some updates in year 2010 *fib* manuals in comparison to year 2004 Eurocode 2.

### 2.4.4 Strut and Tie design in Eurocode 8 and Eurocode 4.

The consideration of inclined compression struts bearing on transverse plates intervening in the equilibrium was first made explicit, in a normative context, in the frame of background research activity to Eurocode 8 or EN1998-1-1:2004. The complete background activity is reported in the ICONS research report (PLUMIER, 2001). The corresponding normative expressions for the strength of concrete compression struts bearing on plates which are part of a steel section are given in the normative Annex C of Eurocode 8 and mentioned as a “mechanism 2” consisting of compressed concrete struts inclined to the column sides (Figure 2.4.4).

When no façade steel beam is present, the moment capacity of the joint may be calculated from the compressive force developed by the combination of the following two mechanisms:

mechanism 1: direct compression on the column. The design value of the force that is transferred by means of this mechanism should not exceed the value given by the following expression:  $F_{Rd1} = b_b d_{eff} f_{cd}$

mechanism 2: If the angle of inclination is equal to  $45^\circ$ , the design value of the force that is transferred by means of this mechanism should not exceed the value given by the following expression:

$$F_{Rd2} = 0,7 h_c d_{eff} f_{cd}$$

where  $h_c$  is the depth of the column steel section.

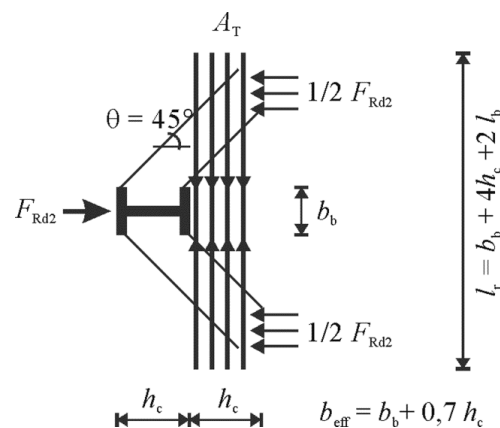


Figure 2.4.4: Figure C2(e) of EN1998-1-1

## CHAPTER: THREE

### RESEARCH METHODOLOGY

#### 3.1 Materials:

A brief description of the constituent materials as used in the present investigation is given below

##### 3.1.1 Concrete:

Concrete (C40/50)

- Characteristic strength  $f_{ck} = 40$  MPa;
- Mean value of Elastic modulus  $E_{cm} = 35000$  MPa;

And in FEM software the stress-strain relationship for concrete is define according to Popovics (1973). As shown in Figure 000, these curves reflect the greater stiffness and linearity of the ascending branch and the reduced ductility of concretes as the peak compressive stress increases. The stress-strain curve is given by the following equation:

$$f_{ci} = -\left(\frac{\varepsilon_{ci}}{\varepsilon_p}\right) f_p \frac{n}{n-1 + \left(\frac{\varepsilon_{ci}}{\varepsilon_p}\right)^n} \quad \text{for } \varepsilon_{ci} < 0$$

The long fraction represents the deviation from linear-elastic response. The curve fitting parameter,  $n$ , captures the greater linearity of higher strength concrete through the diminishing difference between the initial tangent stiffness  $E_c$ , and secant stiffness,  $E_{sec}$ . These values are computed as follows:

$$n = \frac{E_c}{E_c - E_{sec}}$$

$$E_{sec} = \frac{f_p}{|\varepsilon_p|}$$

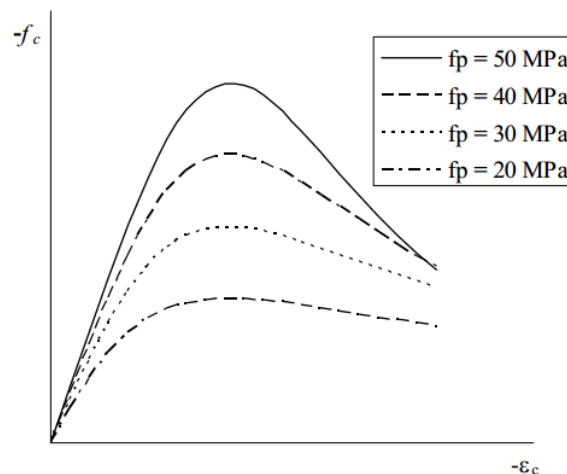


Figure 3.1.1: Popovics pre- and post-peak concrete compression responses

### 3.1.2 Steel Profile:

Steel profile: HE 120 B

Dimension:  $W=H= 120\text{mm}$

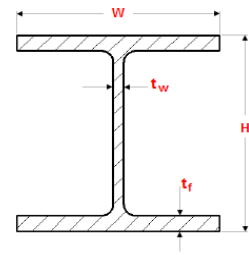
Grade Designation: S355

$t_w = 6.5\text{mm}$

Min. Yield Strength :  $355\text{ N/mm}^2$

$t_f = 11\text{mm}$

Mod. of Elasticity,  $E_a = 210000\text{ MPa}$



The stress-strain relationship for steel class S355 with bi-linear law for non-linear analyses,

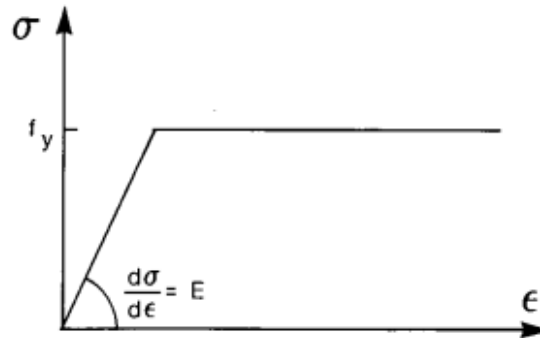


Figure 3.1.2: Bi-linear stress-strain relationship

### 3.1.3 Reinforcement

Diameter:  $\Phi_1 = 10\text{ mm}$  diameter of longitudinal reinforcement

$\Phi_1 = 12\text{ mm}$  diameter of horizontal reinforcement

Grade Designation: S355

Min. Yield Strength:  $355\text{ N/mm}^2$

Mod. of Elasticity,  $E_a = 200000\text{ MPa}$

And the stress strain relationship for reinforcement is also bi-linear (Figure 3.1.2).

### **3.2 Specimen Details:**

All the specimens and their configuration are described briefly here,

#### **3.2.1 Concrete wall**

The necessary thickness B of the wall is defined as:

$$\begin{aligned} B_{\text{nec}} &= 2 \cdot c_v + 2 \cdot \phi_1 + h_{\text{HE120B}} + 2 \cdot h_{\text{sc}} \\ &= 2 \cdot 35\text{mm} + 2 \cdot 10\text{mm} + 120\text{mm} + 2 \cdot 65\text{mm} = 340\text{mm}; \end{aligned}$$

where:

$c_v = 35$  mm – concrete cover;

$\Phi_1 = 10$  mm – longitudinal reinforcement;

$h_{\text{sc}} = 65$  mm – shear stud height;

$H = 1000$  mm – concrete wall height;

$D = 1000$  mm – concrete wall length

The failure of the concrete wall shall not take place as:

$$40\text{MPa} \cdot (340\text{mm} \cdot 1000\text{mm} - 160\text{mm} \cdot 160\text{mm}) = 13587\text{kN}$$

160mm x 160mm – polystyrene cross-section dimension.

#### **3.2.2 Embedded steel profile – HE 120B**

The maximum compressive axial force is limited by the plastic design resistance of the embedded steel profile.

$$\text{For a HE 120 B profile: } N_{\text{pl,Rd}} = \frac{A_{\text{HE120B}} \cdot f_{\text{ay}}}{\gamma_{\text{Mo}}} = \frac{3400\text{mm}^2 \cdot 355\text{MPa}}{1} = 1207\text{kN}$$

#### **3.2.3 Configuration A and C (stud connector):**

The cross-sections for Configurations A and C are presented in Figure 3.2.3. Long connections with flexible connectors are chosen to make the load transfer. A polystyrene block is provided at the end of steel profile. In configuration A, the steel profile strong axis is perpendicular to wall face. To prevent longitudinal splitting by shear studs, links are provided under the head of each shear stud. In configuration C, the steel profile weak axis is perpendicular to the wall face



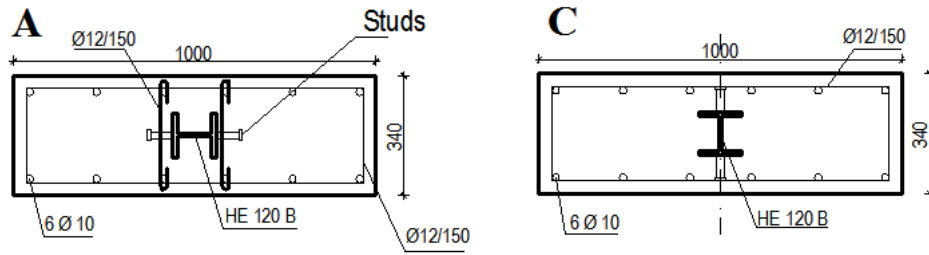


Figure 3.2.3: Configuration A and C.

### 3.2.4 Configuration B and D (Plate connector):

Cross-section definitions for Configuration B and D are given in Figure 3.2.4. In these cases, welded internal bearing plates are used as connectors and in this case direct bearing of concrete compression struts is used to transfer loads from concrete to steel. Here B and D have the configuration without ties to equilibrate the compression struts. The material properties and concrete wall dimensions are kept the same as in Configuration A and C. A polystyrene block equal with 100 mm is provided at the end of steel profile.

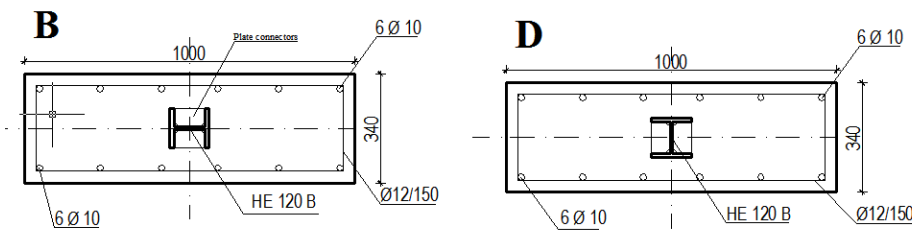


Figure 3.2.4: Configuration B and D.

### 3.2.5 Configuration E (Studs and plate connector):

Configuration E combines flexible and stiff connectors as shown in Figure 3.2.5. The steel profile has the weak axis perpendicular to wall face. The embedment length is kept the same as previous configurations, equal to 900 mm, as shown in Figure 10.

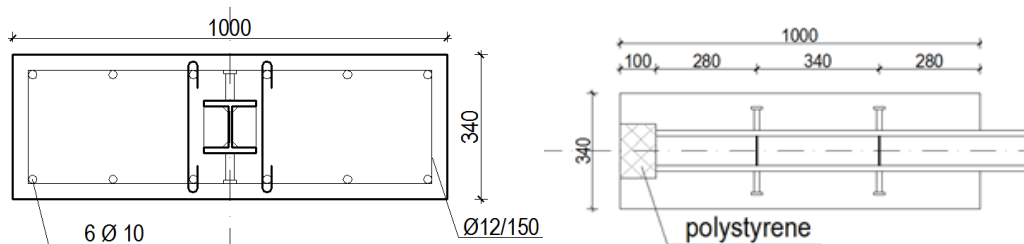


Figure 3.2.5: Configuration E

### **3.3 FEM Software:**

In this study for numerical analysis of the specimen here VecTor2.0 program is used. VecTor2.0 is a program for nonlinear analysis of two-dimensional reinforced concrete membrane structures. This program has been developed at the University of Toronto. VecTor2.0 is a program based on the Modified Compression Field Theory for nonlinear finite element analysis of reinforced concrete membrane structures. Considering the inherent intricacies of nonlinear finite element analysis and VecTor2, user facilities are imperative to their rational and convenient application.

Non-linear finite element procedures currently represent the most complex and advanced tools for predicting the response of reinforced concrete structures. They incorporate models from various constitutive frameworks such as non-linear elasticity, plasticity, continuum damage mechanics, smeared fixed/rotating crack models, micro plane models (CEB-FIP, 2008). Each of these approaches has proven effective in some applications and less effective in others. VecTor2 is a finite element program for 2D static and dynamic analysis of reinforced concrete structures. It has been developed over the last 18 years by Prof. Vecchio and his research group at the University of Toronto. Used in this study is VecTor2, Revision 6.0 from the 8<sup>th</sup> of February, 2008. The basic models implemented into the program include the Modified Compression Field Theory (MCFT – Vecchio and Collins, 1986) and the Disturbed Stress Field Model (DSFM – Vecchio, 2000). Both the MCFT and the DSFM fall into the category of smeared rotating crack models, as later is built on the concepts of the former. The main difference between the DSFM and the MCFT lies in the reorientation of the stress and strain fields. The basic assumption of the MCFT is that the average direction of the principal compressive stresses coincides with the average direction of the principal compressive strains and that the critical cracks are parallel to this direction. In contrast, the DSFM explicitly accounts for slip deformations at the critical cracks which results in delayed rotation of the stress field with respect to the strain field. The critical cracks in the DSFM are kept perpendicular to the direction of the principal tensile stresses.

## CHAPTER: FOUR

### DESIGN AND NUMERICAL MODELING

#### 4.1 Theoretical Design:

In this section, the theoretical design of all the specimens is briefly described. As in all the specimens the same concrete section and steel profile is used, so their capacity remains the same. The capacity of concrete is 13587kN and plastic resistance of the embedded steel profile is 1207kN. The design capacity of each specimen is taken in design is  $N_{\max} = 1000\text{kN}$ , in order to achieve the failure in the load transferring mechanism. Details designs are described below.

##### 4.1.1 Configuration A and C (stud connector):

###### **Shear studs characteristics:**

Geometrical characteristic of the shear studs

$d = 16 \text{ mm}$  – diameter of the shear stud;

$h_{sc} = 65 \text{ mm}$  – stud height;  $3d = 48 \text{ mm} \leq h_{sc}$  ;

$s_c = 200 \text{ mm}$  – longitudinal spacing;  $5d = 80 \text{ mm} \leq s_c \leq \min(6h_{sc}; 800\text{mm})=390\text{mm}$ ;

$f_u = 500 \text{ MPa}$  – maximum stud tensile strength;

###### **Shear connector strength:**

EC 4.1.- §6.6.3.1. (1) gives the individual shear connector characteristic strength:

$$P_{Rk} = \min \left( \frac{0.8 \cdot f_u \cdot \pi \cdot d^2 / 4}{\gamma_v}, \frac{0.29 \cdot \alpha \cdot d^2 \cdot \sqrt{f_{ck} \cdot E_{cm}}}{\gamma_v} \right) = 80.43\text{kN}$$

Where,

$d = 16 \text{ mm}$ – shear stud diameter;

$h_{sc} = 65\text{mm}$

$f_u = 500\text{MPa}$ ;

$f_{ck} = 40\text{Mpa}$ ;

$\gamma_v = 1.00$ ;

$$\alpha = \begin{cases} 0.2 \left( \frac{h_{sc}}{d} + 1 \right) & \text{for } 3 \leq \frac{h_{sc}}{d} \leq 4 \\ 1 & \text{for } \frac{h_{sc}}{d} > 4 \end{cases} = 1;$$

The necessary number of shear studs is:  $\frac{N_{max}}{P_{Rk}} = \frac{1000\text{kN}}{80.43\text{kN}} = 12.43$ .

The strength capacity of  $n_{studs} = 12$  shear studs is equal to:  $N_{Rd} = n_{studs} \cdot P_{Rk} = 965.1 \text{ kN}$ . The distance between two shear studs is equal to:  $s_c = 150\text{mm}$ .

The design resistance of the shear studs connection is:

$$N_{Rd} = 965.1 \text{ kN} < N_{max} = 1000 \text{ kN}.$$

Reinforcement design and strut and tie model are explained in Annex: ASP1.

#### **4.1.2 Configuration B and D (plate connector):**

##### **Plate connector characteristics**

Plate connectors are welded to the web of the steel profile HE 120B shape. They have the following geometrical characteristics :

- Width of the plate:  $a = \frac{b_f - t_w}{2} = 56.75\text{mm}$
- Length of the plate:  $b^* = h - 2 \cdot t_f = 98\text{mm}$
- Width of the clipped corners:  $c = 15\text{mm}$
- Area:  $A_{plate} = a \cdot b - c^2 = 53.36\text{cm}^2$

##### **Plate connector strength**

The plate connector strength is determined considering the following strut & tie model, as shown in Figure 4.1.2. It is considered that the struts are formed assuming an angle  $\alpha = 45^\circ$ .

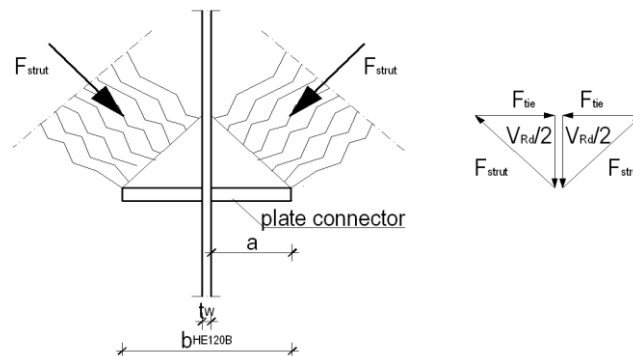


Figure 4.1.2: Strut & tie model to determine plate connector strength.

Strut width is equal to:  $\frac{a}{\cos \theta} = \frac{a}{\frac{\sqrt{2}}{2}} = 80.26\text{mm}$

The strut resistance:  $F_{Rd} = \frac{a}{\sqrt{2}} \cdot \sigma_{Rd,max} \cdot b^* = 158.56\text{kN}$

where:

$$\nu' = 1 - \frac{f_{ck}}{250} = 0.84$$

$$\sigma_{Rd,max} = 0.6 \cdot \nu' \cdot f_{cd} = 20.16\text{MPa}$$

$$f_{cd} = 40\text{MPa}$$

For one plate:

$$V_{Rd,1plate} = F_{Rd} \cdot \cos \theta = 112.12\text{kN}$$

The necessary plate number is:

$$n_{plates} = \frac{N_{max}}{V_{Rd,1plate}} = 8,9$$

The strength capacity of  $n_{plates} = 8$  plate connectors, 4 plates on each side, is equal to:

$$N_{Rd} = n_{plates} \cdot V_{Rd,1plate} = 896.96\text{ kN.}$$

The design resistance of the connection is:

$$N_{Rd} = 896.96\text{kN} < N_{max} = 1000\text{kN.}$$

### Required bearing plate thickness

For rectangular plates supported on three sides, elastic solutions for plate stresses such as those found in Roark's Formulas for Stress and Strain may be used for thickness calculation.

The required bearing plate thickness is determined on the basis of the expression used in Plumier. et al. (2013). The yield lines are not formed at  $45^\circ$ , meaning that the yield line is shorter than  $2a\sqrt{2}$ , as shown in Figure 4.1.3. The actual yield line is:  $b\sqrt{2}+a-b/2 = 77.05\text{ mm.}$

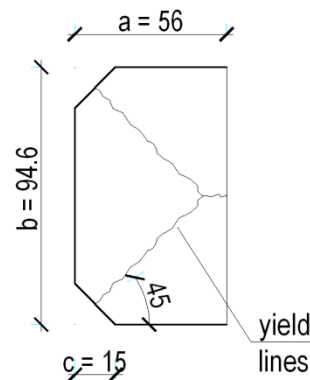


Figure 4.1.3. Internal bearing plate yield line pattern (fixed condition).

The bearing pressure on plate:  $w_u = \frac{V_{Rd,1plate}}{A_{plate}} = 21.01\text{MPa}$

The required bearing plate thickness  $t_p$  is:

$$t_p \geq \frac{2.8 \cdot a}{a + 0.9 \cdot b^*} \sqrt{\frac{2 \cdot a^2 \cdot w_u \cdot (3 \cdot b - 2 \cdot a)}{3 \cdot \phi \cdot f_{ay} \cdot (6 \cdot a + b^*)}} = 8.36\text{mm}$$

Where:

$$\phi = 0.9$$

$$t_p = 9 \text{ mm.}$$

The minimum spacing between two plates is recommended to be:  $s_{p\_min} = 2a + t_p = 137.5 \text{ mm.}$

The maximum spacing is:  $s_{p\_max} = 6a = 340.5 \text{ mm.}$  In order to keep the same embedded distance for the steel profile, as in previous configurations, the distance between two connectors is:  $s_p = 250 \text{ mm.}$

The weld thickness  $a = 5 \text{ mm}$  and follows the condition of  $2a > t_p = 9 \text{ mm}$ , as shown in Figure 4.1.4.

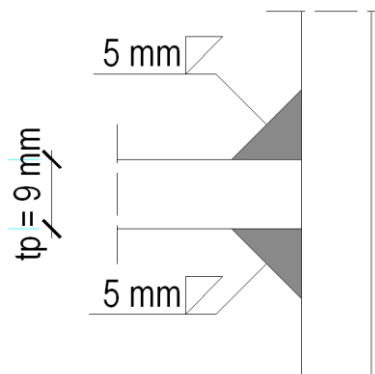


Figure 4.1.4. Weld dimensions of the plate connector.

### Bearing plate strength

Considering the thickness of the plate is 9 mm the bearing pressure of the plate can be calculated by the same way. So bearing pressure for each plate with 9mm thickness,

$$w_u = 25.14\text{MPa}$$

$$\begin{aligned} \text{Each plate load bearing capacity,} &= (25.14 \cdot 94.6 \cdot 56 \cdot 10^{-3}) \text{ kN} \\ &= 133.17 \text{ kN} \end{aligned}$$

$$\begin{aligned} \text{So total bearing plate strength} &= 133.17 \cdot 8 \text{ kN} \\ &= 1065.5 \text{ kN} \end{aligned}$$

Reinforcement design and strut and tie model are explained in Annex: ASP2.

### 4.1.3 Configuration E (studs and plate connector):

It is considered that the compressive axial force  $N_{\max} = 1000\text{kN}$  is resisted by both shear studs and plate connectors. The total number of plate connectors is obtained by the formula:

$$\frac{N_{\max}/2}{V_{\text{Rd},1\text{plate}}} = 4.46$$

where:

$$V_{\text{Rd},1\text{plate}} = 112.12\text{kN}$$

The number of shear studs needed is:  $\frac{N_{\max}/2}{P_{\text{Rk}}} = 6.217$

where:

$$P_{\text{Rk}} = 80.45 \text{ kN};$$

For  $n_{\text{plates}} = n_{\text{studs}} = 4$  the resistance of connectors is:

$$N_{\text{Rd}} = n_{\text{plates}} \cdot V_{\text{Rd},1\text{plate}} + n_{\text{studs}} \cdot P_{\text{Rk}} = 770.18\text{kN}$$

The position of the connectors is shown in Figure 9. The distance between 2 rows of connectors is equal to:  $s_{\text{pc}}=340\text{mm}$ .

the design resistance of the connection is:

$$N_{\text{Rd}} = 770.18 \text{ kN} < N_{\max} = 1000\text{kN}.$$

Considering the plate bearing strength,

$$\begin{aligned} N_{\text{Rd}} &= (4 \cdot 133.17 + 4 \cdot 80.45) \text{ kN} \\ &= 854.5 \text{ kN} \end{aligned}$$

### 4.1.4 Summary:

Summary of all the design forces are listed below in the table 4.1.4.

Specimen	Number of connectors	Shear resistance of 1 connector [kN]	$N_{\text{Rd}}$ [kN]	Expected failure mode
Config.A-SPIA	12 shear studs	80.43	965.10	Connection failure

Config.C- <b>SP1C</b>	12 shear studs	80.43	965.10	Connection failure
Config.B- <b>SPBM1</b> and <b>SPBM2</b>	8 plate connectors	112.12	896.96	Connection failure
Config.D- <b>SPDM1</b> and <b>SPDM2</b>	8 plate connectors	112.12	896.96	Connection failure
Config.E- <b>SPEM1</b>	4 shear studs+ 4 plate connectors	80.43 + 112.12	770.18	Connection failure

Table 4.1.4: Summary of design resistances of specimens



## **4.2 Numerical modeling of the specimens:**

In this section how the numerical modeling of the specimens are described below.

### **4.2.1 Configuration A and C (stud connector):**

As here to analysis the specimen, I use 2D analysis software so it is not possible to model the shear stud as explicit. To simplify the problem here I use reinforcing bar instead of shear stud. And the properties of the steel bar are determined by the properties and behavior of the shear stud. The distance between the steel and concrete surface is close to zero so the bar actually acting vertically. Details are shown in the figure,

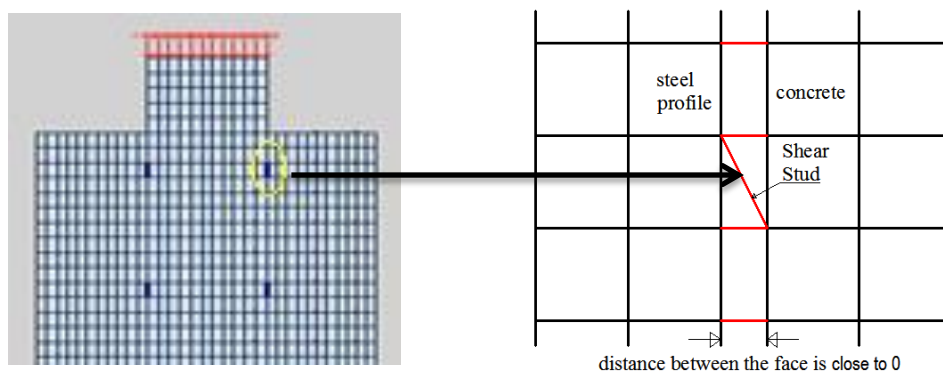


Figure 4.2.1a: Shear studs modeling

As in the design the shear stud capacity already determined, now here we need the load slip relationship to define the behavior of the shear stud. A lot of experimental study has been done to investigate the relation between force and slip in shear studs connection. An extensive parametric study of push-out test specimens with different parameter were also performed experimentally and by using finite element analyses approach. In 2011 Mohammad Makki Abbass, proposed an equation for load-slip relation in his paper on International Journal of Earth Sciences and Engineering (ISSN 0974-5904, Volume 04, No-06 SPL). The slip( $u$ ) is considered as non-dimensional parameter as a ratio of slip( $u$ ) to stud diameter( $d$ ). And here  $Q$  is the load in kN and  $f_{cu}$  is the characteristic strength of concrete.

$$Q=0.0407*(f_{cu})^{0.57} *d^2*((u/d)/(0.01245+(u/d)))$$

In figure 4.2.1 this curve has been plotted and also explained how to get the equivalent reinforcement properties.

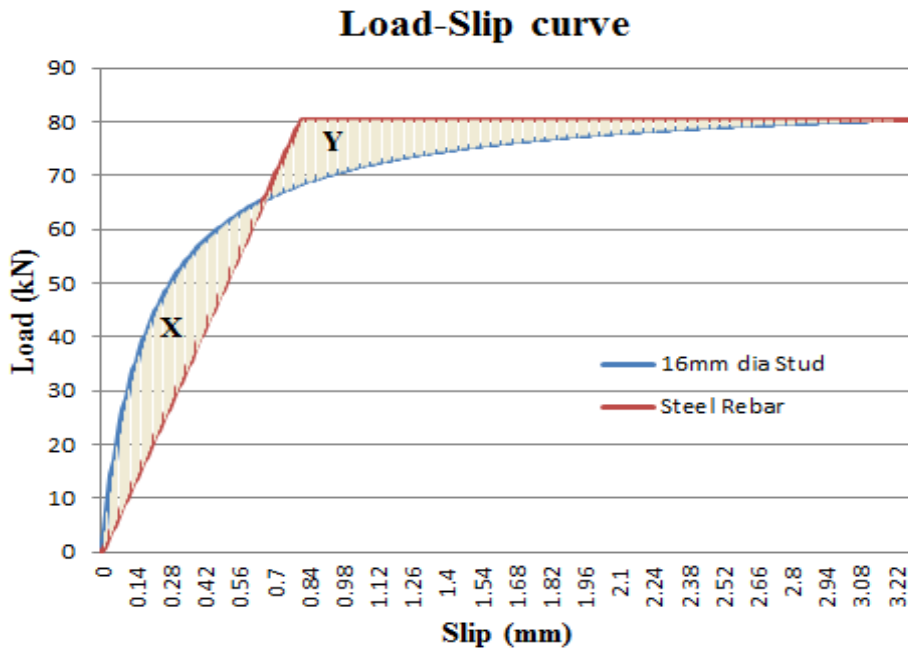


Figure 4.2.1b: Load-slip relationship for shear studs

In this study, diameter of the stud is 16mm; concrete characteristic strength is 40MPa and characteristic strength of individual shear connector 80.45kN. Load-slip curve is explained in the figure 4.2.1. Considering the area X and area Y in the figure 4.2.1 is equal we can determine the stiffness (k) for the rebar.

Now for the rebar to calculate elastic modulus  $E_{rebar}$  and yield strength  $f_y$ ,

$$(E_{rebar} * Area) / Length = \text{Stiffness (k)}$$

$$Area * \text{Strength (} f_y) = \text{Load}$$

In this modeling it is considered that there is no bonding between the steel profile and concrete and they are only connected with the connector.

Details of the specimens with shear stud are summarized in table 4.2.1 below.

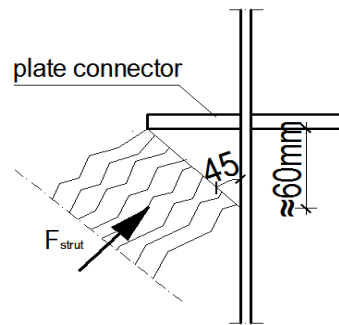
Specimen	SP1A for configuration A	SP1C for configuration C
Details	The steel profile strong axis is perpendicular to wall face and stud is welded with flange.	The steel profile weak axis is perpendicular to wall face and stud is welded with flange and considering thickness 340mm instead 1000mm

Figure		
No of stud connection	12	12
Failure load and mode	965kN in connection failure	965kN in connection failure

Table 4.2.1: Details of Specimen SP1A and SP2C

#### 4.1.2 Configuration B and D (plate connector):

In case of plate connector it is tough to model those specimens in a 2D program as the problem is 3D. So here I proposed some way to model those specimens. In stud and tie model we consider that the load transferred in concrete with  $45^\circ$ . So to simplify the problem, I consider 60mm length of concrete below the connector is perfectly bonded with steel profile.



Now here I proposed couple of ways to model these specimens in VecTor2.0.

##### 4.2.2.1 Model01:

In first case, it is considered that concrete is perfectly bonded 60mm with flange at 190mm spacing, because the spacing between the plates is 250mm. There are 4 bonds of 60mm to represent 4 plates in each side. To define the concrete and steel profile here layer of element one top of another has been used. Now there is a problem with this model is, if I use one layer of material in top of another layer of material then both elements are perfectly bonded in those place. To solve this, the concrete parts where the load expected to transmit are separated from the profile and connected in the bonded part. Now it become like a strip of material which connected in the 60mm bonded zone. So only bonded part is transmitting the load to concrete. In this case, the failure is occurring at the element where they are perfectly

bonded by local crushing. So to prevent this high strength element property is used in that bond zone places. The steel profile will fail by yielding at around 1200kN so to ensure and see the failure of connection, the strength of steel material is increased to 1000MPa. All the reinforcement is designed as smeared reinforcement. Specimen is supported at the bottom. Steel profile and the concrete encaged within the flange dose not continue until the bottom of the specimen but it stopped at 100mm before from the bottom. So at the bottom of the profile is hollow and it is not supported and can move downward. In this case displacement is applied in steel profile at the top.

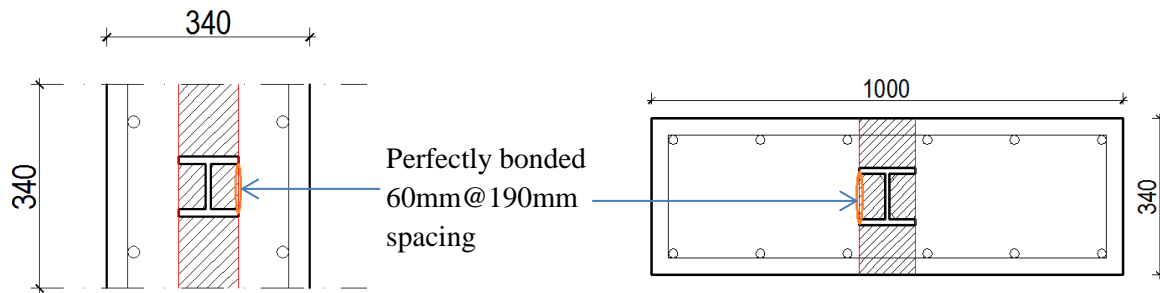


Figure 4.2.2.1: Modeling of specimen SPBM1 and SPDM1

SPBM1: specimen B and finite element modeling is done according to the procedure describe above.

SPDM1: specimen D and finite element modeling is done according to the procedure describe above.

#### 4.2.2.2 Model02:

To simplify the problem and get better result from the program VecTor2.0 only one layer of material is used to model. So in proposed Model02 is define by the layer of concrete and steel profile to transfer load. In the steel profile only flange is define and connected with the plates. The thickness of the flange and plate is 98mm as in the main specimen. Concrete is perfectly bonded with the plate and 60mm with the flange just below the plate. As here only the flange of the steel profile is acting to transfer load from steel to concrete, to ensure failure is not occurring in steel, high strength of steel material is used to define the flange. Now in the concrete part there is a problem with thickness. In this case concrete two concrete thicknesses is used one is 98mm and another is 340 mm. In 98mm it is consider as a strip of the total specimen and in 340mm it is consider as the total thickness of concrete is work to carry the load. This idea is used to model both configuration B and D.

Details of the specimen of Model02 are summarized in the table 4.2.2.2 below.

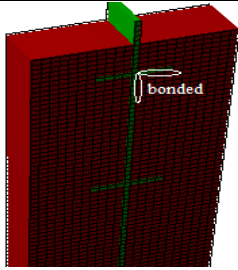
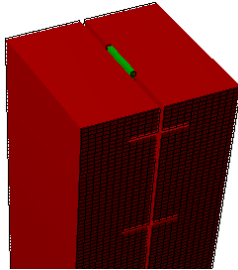
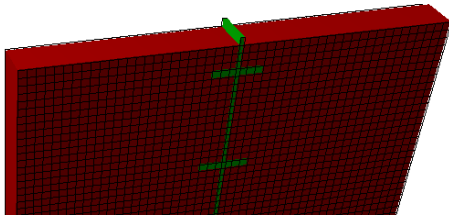
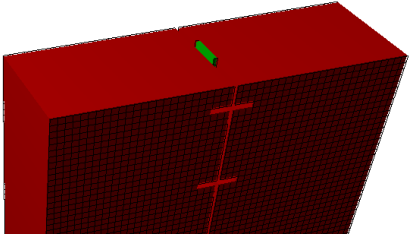
Specimen		Concrete thickness 98mm	Concrete thickness 340mm
SPBM2 for Config.B	Details	Configuration B and FEM modeling is done as Model03.	Configuration B and FEM modeling is done as Model03.
	Figure		
	No. of connection	8	8
	Expected Failure load	897kN	897kN
SPDM2 for Config.D	Details	Configuration D and FEM modeling is done as Model03.	Configuration D and FEM modeling is done as Model03.
	Figure		
	No. of connection	8	8
	Expected Failure load	897kN	897kN

Table 4.2.2.2: Specimen details of SPBM2 and SPDM2

#### **4.2.3 Configuration E (studs and plate connector):**

This specimen has both plate connector and shear stud. It has total 4 plate connector and 4 shear studs, where 2 in each side. In the table 4.2.3 it is explained below. As it has different types of connector and also in different side so to model this specimen in 2D is little bit difficult. So to solve this problem in this proposed model, the specimen for the plate connector and shear studs are modeled separately. The analysis for each type of connector is done in separate model and later calculation is done together to get the combine effect. For

the stud here the modeling of the specimen is done as it is described before in case of specimen A and B. In this case the number of stud is 4 instead of 12. In case of plate, there two ways to model as it explained before. In this case I follow the proposed Model01 for modeling the plate connector; difference is the number of plate is 4 instead of 8.

Details of the specimen of configuration E are summarized in the table 4.2.3 below.

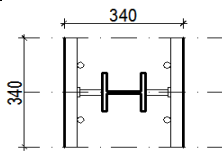
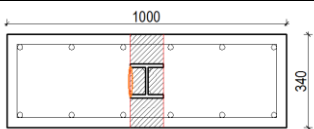
Specimen		With stud	With plate connector
SPEM1 for Config. E	Details	The steel profile weak axis is perpendicular to wall face and stud is welded with flange and considering thickness 340mm instead 1000mm	4 plate connector according. 2 in each side having 340mm spacing.
	Figure		
	No. of connection	4	4
	Expected Failure load	771kN	

Table 4.2.3: Specimen details of SPEM2

## CHAPTER: FIVE

### RESULT AND INTERPRETATION

In this chapter result from the numerical analysis is described and explained. And the also the data obtained from the results are also interpreted and compared with the expected result. For this the post processor for VecTor2.0 called Augustus is used.

#### 5.1 Configuration A and C (shear stud):

##### 5.1.1 Configuration A: (SP1A)

In modeling of this specimen the yield strength of the rebar, which is used instead of shear studs, is used 400MPa. In the result it shows that the failure occurs by yielding of that rebar's. The result from program is shown in the figure below.

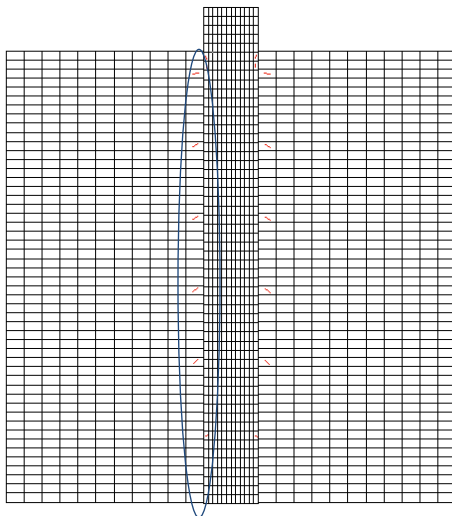


Figure 5.1.1a: cracked view

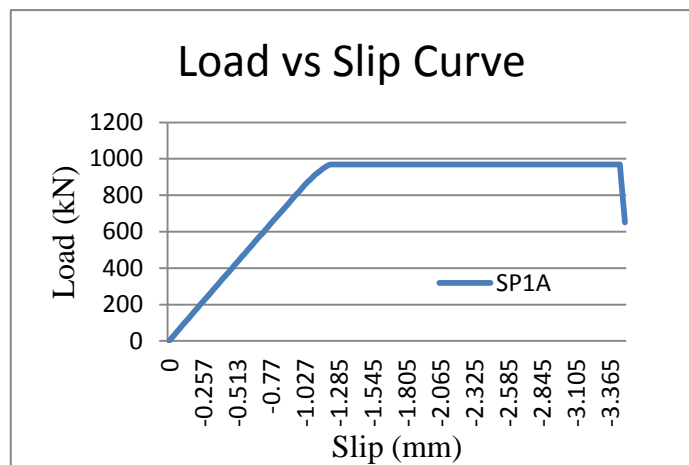
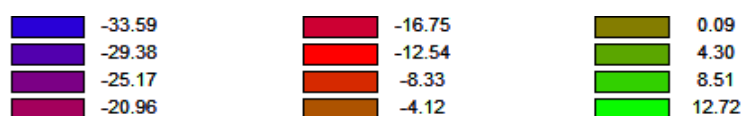


Figure 5.1.1b: load-slip relationship

The graphical results from the FEM program are represented below.

#### **Total stresses: (MPa)**



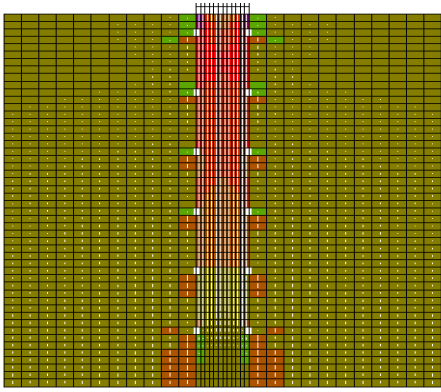


Figure 5.1.1c: vertical stress

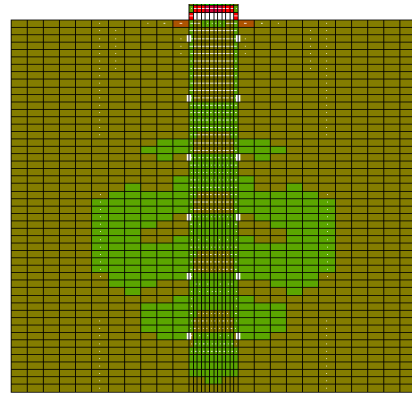


Figure 5.1.1d: horizontal stress

**Stresses in reinforcement: (MPa)**

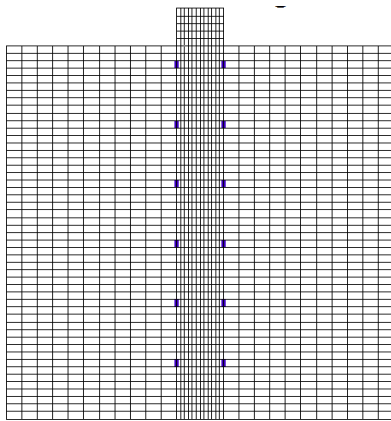


Figure 5.1.1e: stress in studs

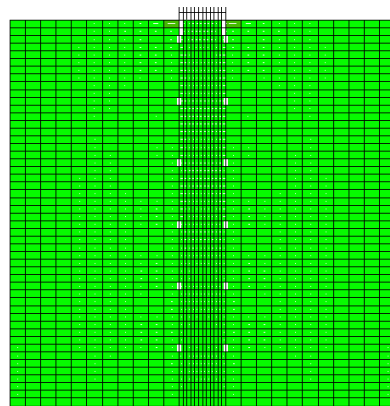


Figure 5.1.1f: stress in smeared rebar

**Stresses in steel profile: (MPa)**

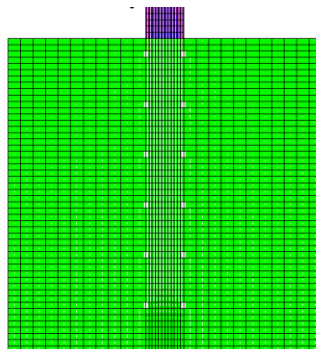
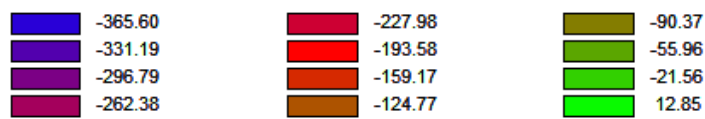


Figure 5.1.1g: vertical stress



From the result above it's clearly seen that the stresses in concrete are much lower than the concrete strength even though there is some crack generate. So it is obvious that the failure will be in the connection. Total restraining force is 970kN. The stresses in smeared reinforcement are also less than its capacity. In steel profile some elements are close to yield at the top free part but it does not fail by yielding.

### 5.1.2 Configuration C (SP1C)

In this case also, in modeling the yield stress for the rebar which is used instead of shear studs is 400MPa. In the result it shows that the failure occurs by yielding of that rebar's.

The result from program is shown in the figure below.

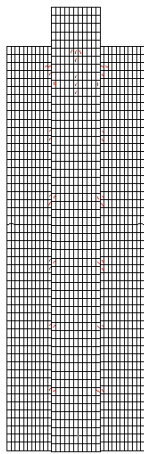


Figure 5.1.2a: cracked view

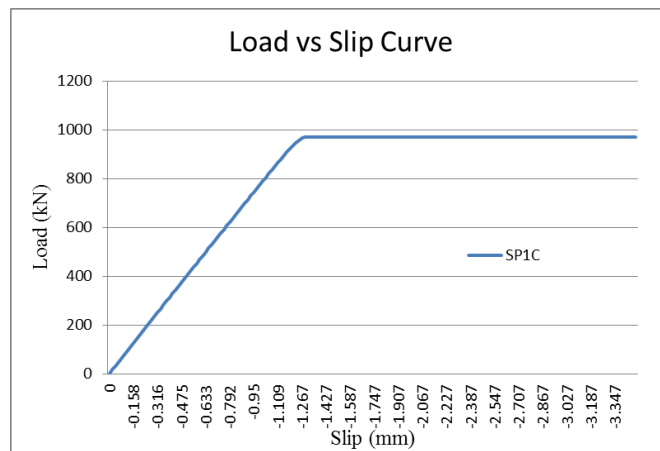


Figure 5.1.2b: load-slip relationship

The graphical results from the FEM program are represented below.

**Total stresses: (MPa)**

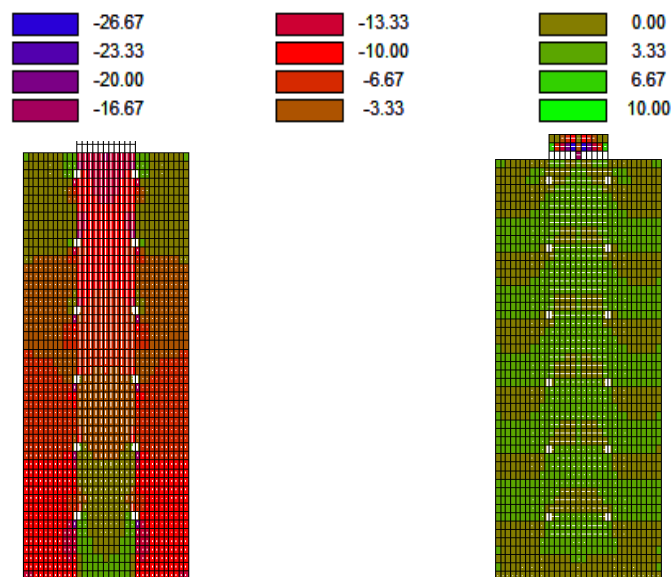


Figure 5.1.2c: vertical stress

Figure 5.1.2d: horizontal stress

### Stresses in reinforcement: (MPa)

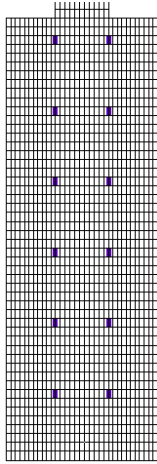
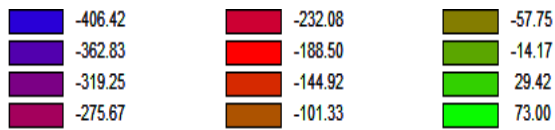


Figure 5.1.2e: stress in studs

### Stresses steel profile: (MPa)

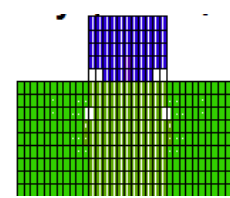
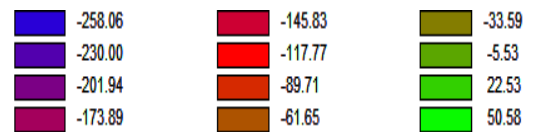


Figure 5.1.2g: vertical stress

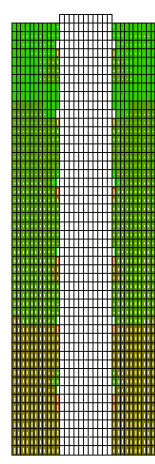


Figure 5.1.2f: stress in smeared rebar

From the result above it's clearly seen that the stresses in concrete are much lower than the concrete strength even though there is some crack generate. So it is obvious that the failure will be in the connection. Total restraining force is 970kN. The stresses in smeared reinforcement are also less than its capacity. In steel profile stresses are also less than its yield stress.

### 5.1.3 Summary:

From above result after interpretation following statements can be stated,

- The main finding can be, to justify if the concrete fails before the studs. As the stresses in concrete are less than its capacity so it is clear that the failure will be in the stud connection.
- In this way we cannot determine the exact total restraining force but we can have an idea about failure.
- We can have an idea about the crack pattern and stresses in concrete due to the load transfer by the shear studs.
- Here we can see that the concrete stress in specimen C is higher than the stresses in specimen A because of the length of the concrete section on which load is transferred. In case A it is longer so stress is less and vice-versa for C.
- Here it is consider that there is no bond between concrete and steel profile but in real case steel profile is encased in concrete, so it is expected more restraining force.

## 5.2 Configuration B and D (plate connector):

### 5.2.1 Model01:

In this case total vertical restraining force for configuration B is 1027kN and Configuration D is 1629kN. Failure occurred in concrete and the crack developed at the bottom and top of the specimen close to the steel profile.

The results from the analysis are shown in the table 5.2.1.

Specimen	Configuration B (SPBM1)	Configuration D (SPDM1)																																																															
Failure load	1027kN	1629kN																																																															
Load-slip curve	<table border="1"> <caption>Approximate data points from the Load-slip curve graph</caption> <thead> <tr> <th>Slip (mm)</th> <th>SPBM1 Load (kN)</th> <th>SPDM1 Load (kN)</th> </tr> </thead> <tbody> <tr><td>0</td><td>0</td><td>0</td></tr> <tr><td>-0.048</td><td>100</td><td>150</td></tr> <tr><td>-0.095</td><td>200</td><td>300</td></tr> <tr><td>-0.144</td><td>300</td><td>450</td></tr> <tr><td>-0.192</td><td>400</td><td>600</td></tr> <tr><td>-0.24</td><td>500</td><td>750</td></tr> <tr><td>-0.288</td><td>600</td><td>900</td></tr> <tr><td>-0.336</td><td>700</td><td>1050</td></tr> <tr><td>-0.384</td><td>800</td><td>1200</td></tr> <tr><td>-0.432</td><td>900</td><td>1350</td></tr> <tr><td>-0.485</td><td>950</td><td>1200</td></tr> <tr><td>-0.533</td><td>1000</td><td>1250</td></tr> <tr><td>-0.583</td><td>1000</td><td>1300</td></tr> <tr><td>-0.632</td><td>1027</td><td>1350</td></tr> <tr><td>-0.681</td><td>1000</td><td>1400</td></tr> <tr><td>-0.729</td><td>900</td><td>1450</td></tr> <tr><td>-0.778</td><td>800</td><td>1500</td></tr> <tr><td>-0.829</td><td>-</td><td>1600</td></tr> <tr><td>-0.878</td><td>-</td><td>1629</td></tr> <tr><td>-0.95</td><td>-</td><td>1300</td></tr> </tbody> </table>		Slip (mm)	SPBM1 Load (kN)	SPDM1 Load (kN)	0	0	0	-0.048	100	150	-0.095	200	300	-0.144	300	450	-0.192	400	600	-0.24	500	750	-0.288	600	900	-0.336	700	1050	-0.384	800	1200	-0.432	900	1350	-0.485	950	1200	-0.533	1000	1250	-0.583	1000	1300	-0.632	1027	1350	-0.681	1000	1400	-0.729	900	1450	-0.778	800	1500	-0.829	-	1600	-0.878	-	1629	-0.95	-	1300
Slip (mm)	SPBM1 Load (kN)	SPDM1 Load (kN)																																																															
0	0	0																																																															
-0.048	100	150																																																															
-0.095	200	300																																																															
-0.144	300	450																																																															
-0.192	400	600																																																															
-0.24	500	750																																																															
-0.288	600	900																																																															
-0.336	700	1050																																																															
-0.384	800	1200																																																															
-0.432	900	1350																																																															
-0.485	950	1200																																																															
-0.533	1000	1250																																																															
-0.583	1000	1300																																																															
-0.632	1027	1350																																																															
-0.681	1000	1400																																																															
-0.729	900	1450																																																															
-0.778	800	1500																																																															
-0.829	-	1600																																																															
-0.878	-	1629																																																															
-0.95	-	1300																																																															
Crack pattern																																																																	

Table 5.2.1: FEM analysis result for SPBM1 and SPDM1

The graphical results from the FEM program are represented below.

**Total stresses: (MPa)**

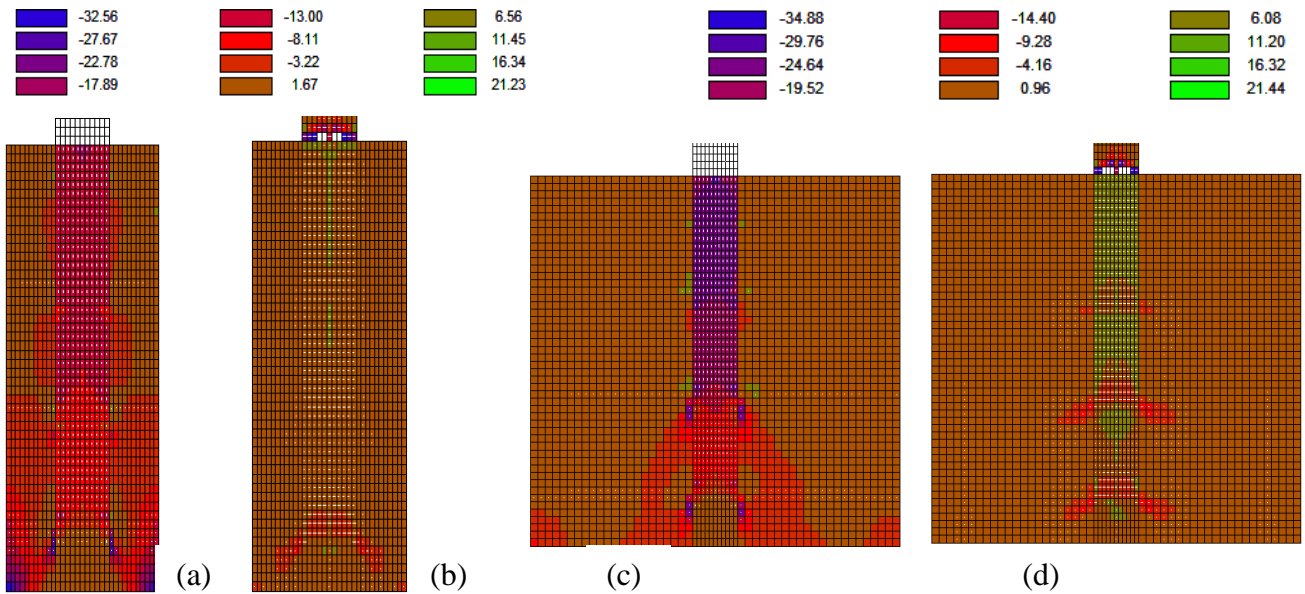


Figure 5.2.1: (a) vertical and (b) horizontal stress for SPBM1, (c) vertical and (d) horizontal stress for SPDM1

**Reinforcing bar stresses: (MPa)**

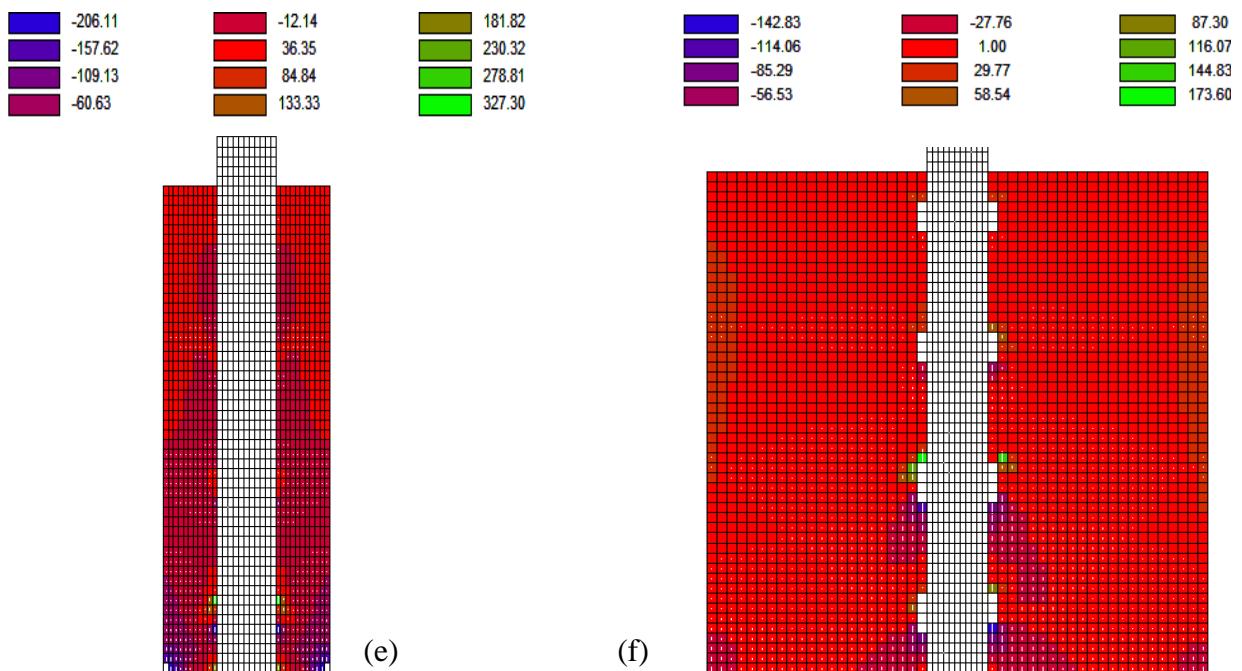


Figure 5.2.1: (e) vertical stress for SPBM1, (f) vertical stress for SPDM1

**Steel profile stresses:**

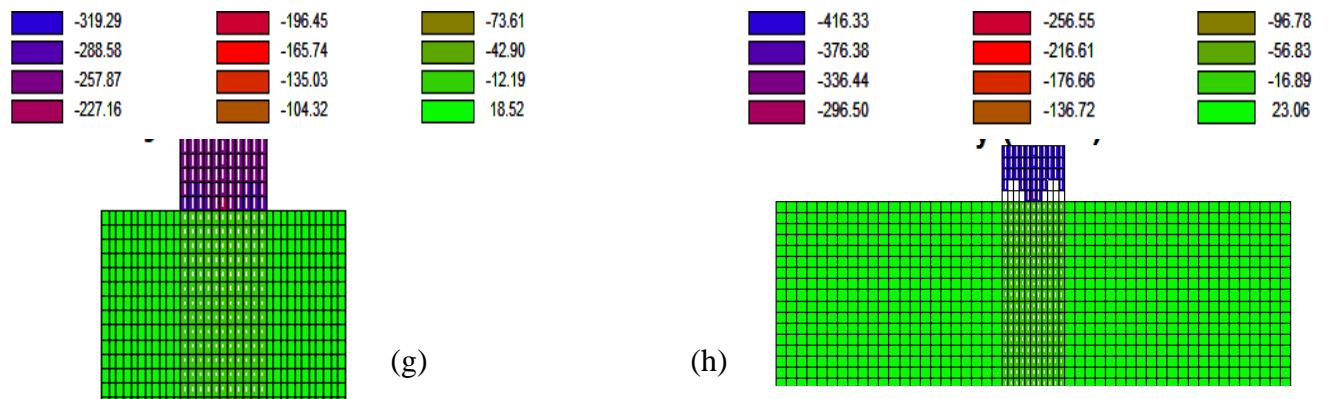


Figure 5.2.1: (g) vertical stress for SPBM1, (h) vertical stress for SPDM1

From the result above its clearly seen that the stresses reinforcement is much lesser than its strength and stresses in concrete is considerable higher in the cracked zone. So in both case the failure is occurring in concrete. In case of B, failure load is less than steel profile yielding but in case of D if we use S355 grade steel the failure will be in steel profile. In both failure can be occurred crushing the concrete at the bottom close to the profile where it is supported. In case of specimen D it also exceeded the capacity of steel plate so in both case also there is a probability of failure occurring in steel plate itself.

**5.2.2 Model02:**

In this case in modeling two types of concrete thickness is used for each configuration. For configuration B the failure load is much lesser then the expected. Specimen with 98mm thickness fails at around 350kN and 340mm is in around 700kN vertical forces. Failure occurs in concrete by creating vertical cracks.

The results from the analysis of configuration B are shown in the table 5.2.2a

Specimen		98mm thickness of concrete	340mm thickness of concrete
SPBM2	Failure load	348kN	697kN

for Config. B	Load-slip curve		
	Crack pattern		

Table 5.2.2a: FEM analysis result for SPBM2

The graphical results from the FEM program are represented below.

**Total stresses:** (MPa)

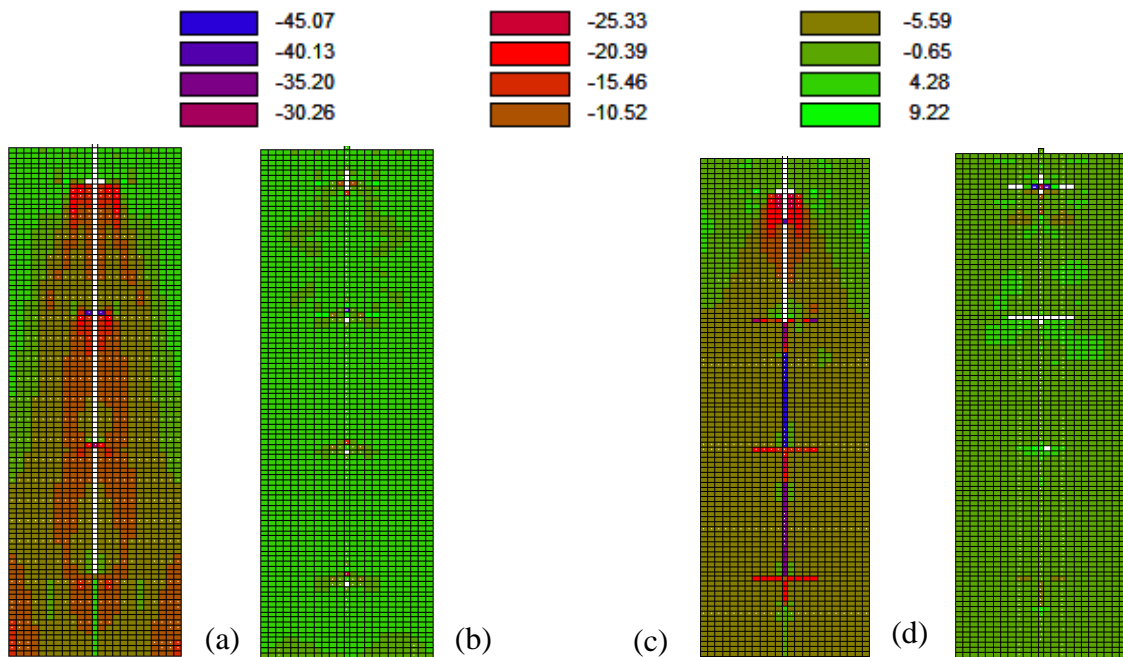


Figure 5.2.2: (a) vertical and (b) horizontal stress for 98mm, (c) vertical and (d) horizontal stress for 340mm

**Stresses in reinforcement: (MPa)**

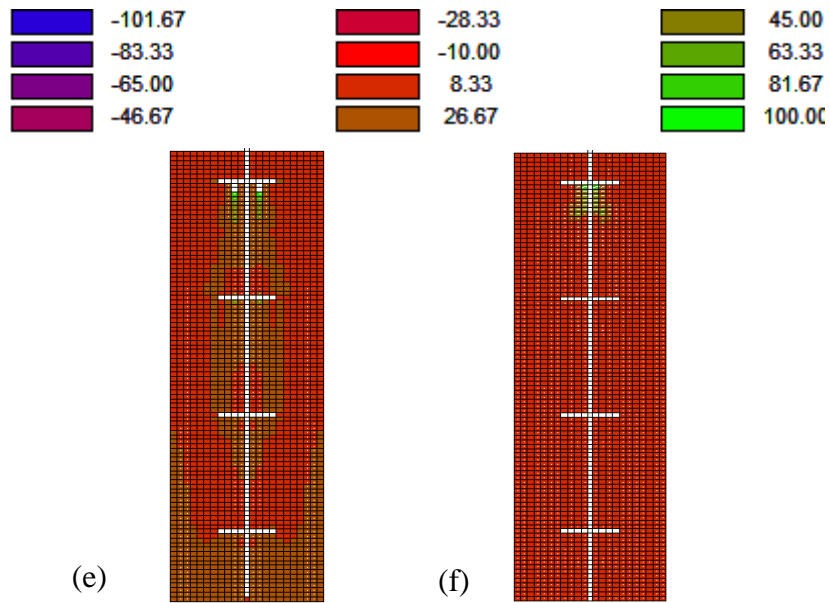


Figure 5.2.2: (e) stress in steel for 98mm, (f) stress in steel for 340mm

From the above results, it's clearly seen that there is a vertical crack generates in the concrete and its split the concrete to fail. If we consider average then the failure load can be around 550kN. The stress distribution in the concrete steel rebar has been shown. In this case the failure load is less than actual steel profile yielding for both 98mm and 340mm thickness of concrete. And the failure is accruing due to the failure in concrete as the stresses in rebar are much lesser than its strength. The elements just below the frist plate connector are in higher stresses.

For configuration D, specimen with 98mm thickness fails at around 1090kN and 340mm is in around 1960kN vertical forces. Failure occurs in concrete by creating vertical cracks.

The results from the analysis of configuration D are shown in the table 5.2.2b

Specimen		98mm thickness of concrete	340mm thickness of concrete
SPDM2 for Config. D	Failure load	1092kN	1957kN

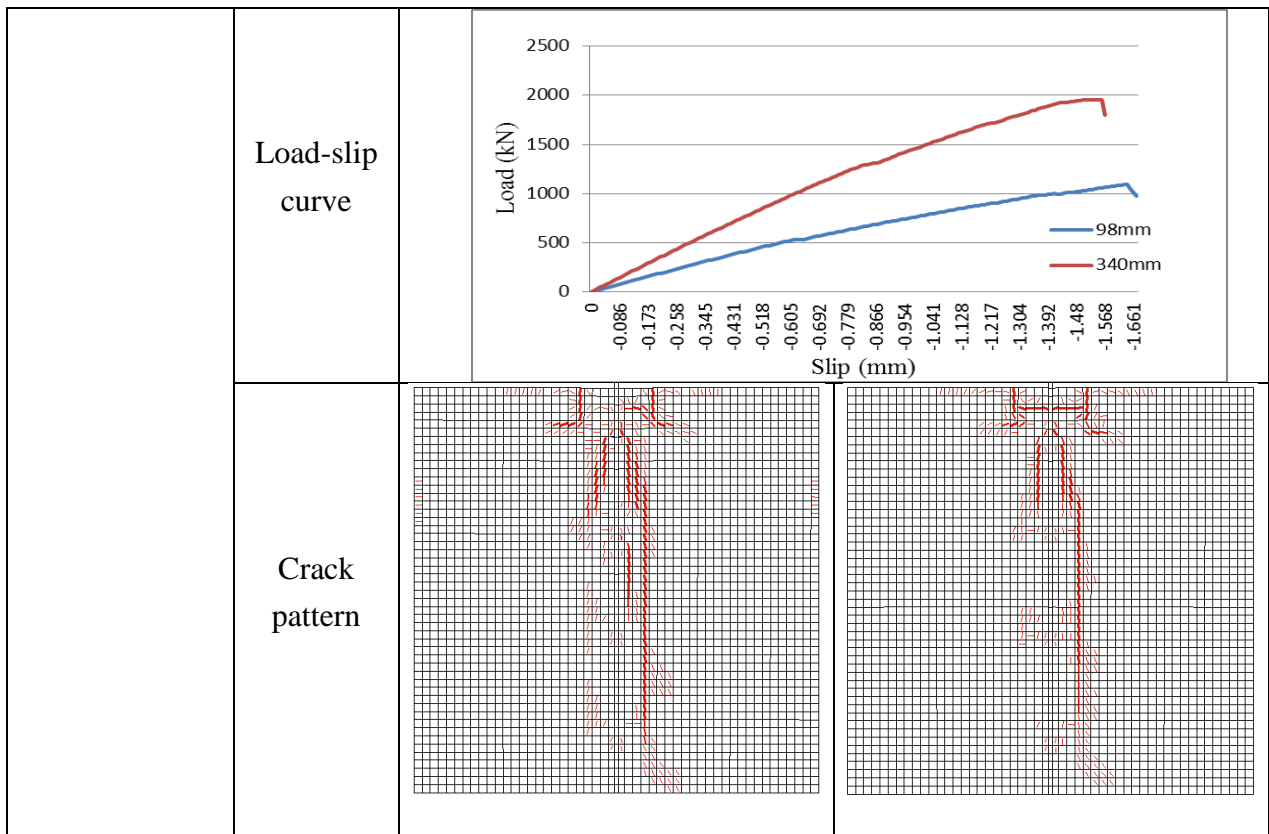


Table 5.2.2b: FEM analysis result for SPDM2

The graphical results from the FEM program are represented below.

**Total stresses:** (MPa)

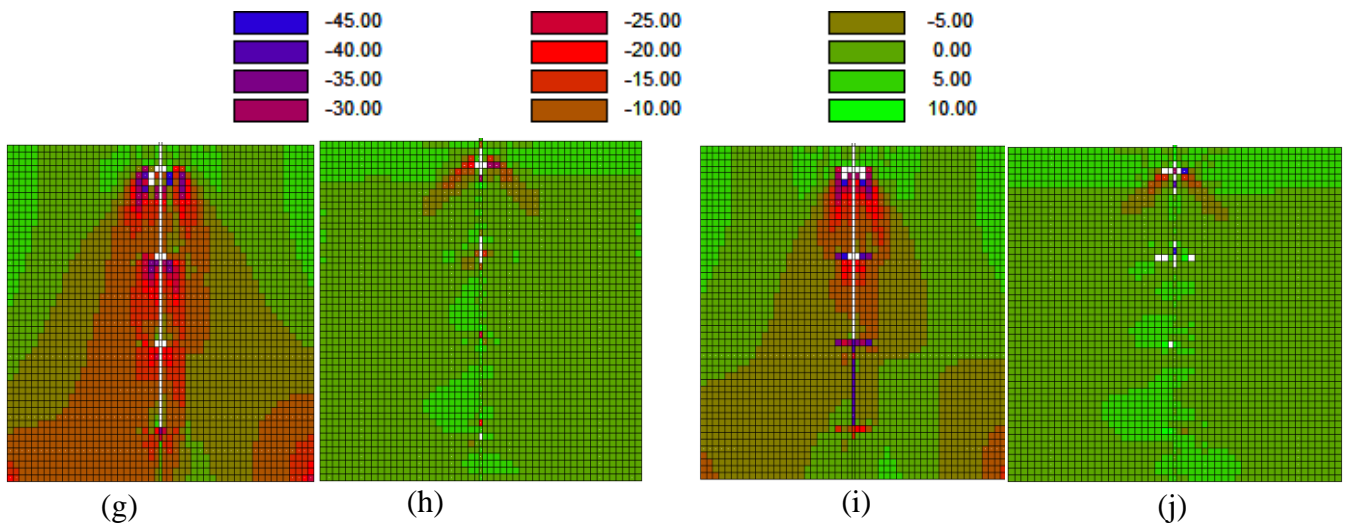


Figure 5.2.2: (g) vertical and (h) horizontal stress for 98mm, (i) vertical and (j) horizontal stress for 340mm

**Stresses in reinforcement:** (MPa)



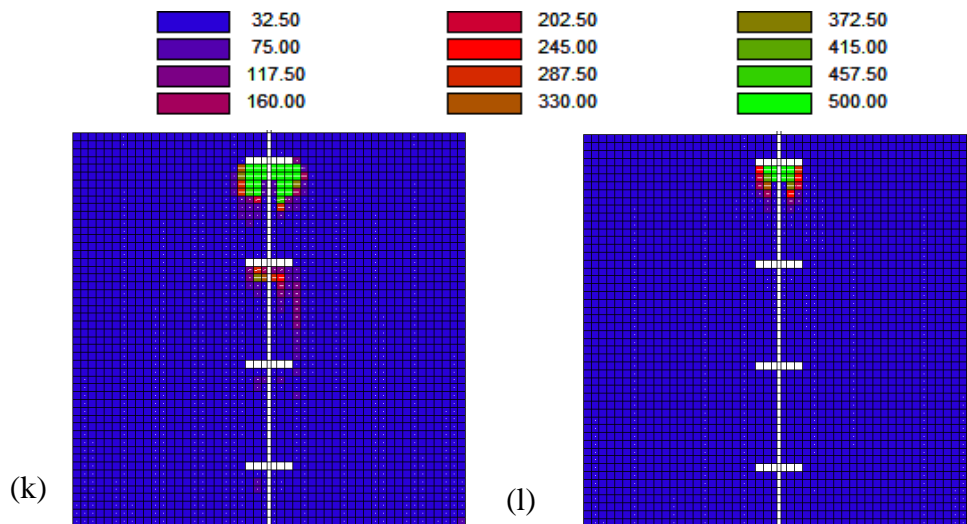


Figure 5.2.2: (k) stress in steel for 98mm, (l) stress in steel for 340mm

In this case, concrete width is nearly 4 times then previous. And there is also a vertical crack generates in the concrete and its split the concrete to fail. The stress distribution in the concrete steel rebar has been shown. In this case the average failure load is more or less 1500kN. And the stresses in rebar are exceeding their strength just below the plate and also the stresses in concrete are also higher than its capacity.

In these cases also the force exceeded the bearing capacity of steel plate so in both cases also there is a probability of failure occurring in steel plate itself.

### 5.2.3 Summary:

From above result after interpretation following statements can be stated,

- In most of the case obtained restraining vertical forces are higher than the expected load
- Most of the case concrete fails before the stresses in reinforcement is reach to its yield stress. So in struts and tie model, it can be assume that the concrete will fail before the reinforcement reach its tension capacity.
- As in configuration D the width of the concrete where the load transmits is bigger than configuration B, so the restraining force is also higher in configuration D in all cases.
- In all case concrete section are considered separate but in real case they are connected and encased the steel profile. So it is expected in real case restraining force will be much higher.

- As modeling is done in 2D program so the property is not define in other dimension. The results obtained from this numerical study are not exactly perfect but it gives an idea about the failure.

### 5.3 Configuration E (studs and plate connector):

In this case as explained before both stud and plate connector are modeled separate. The plate connectors are stiffer then shear studs. So from the load-slip curve it is clear that specimen with plate connector fail at very high restraining force but in small slip value. On the other hand specimen with stud fails at high slip value. Now for the combine effect, it is consider that the failure of the specimen is occurred at the same slip value when the specimen with plate connector fails. So the total restraining force is the sum of the failure load of plate connectors and load corresponding to the same slip value for stud failure. In this case failure load is around 1300kN. The results from the analysis of configuration E are shown in table 5.3.

Specimen	SPEM1 for configuration E	
Failure load	1295kN	
Load-slip curve		

Table 5.3: FEM analysis result for SPEM2

The graphical results from the FEM program are represented below.

**Total stresses: (MPa)**

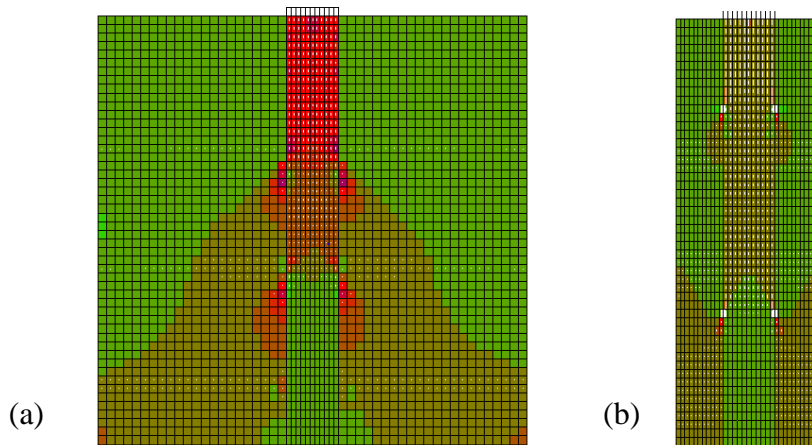
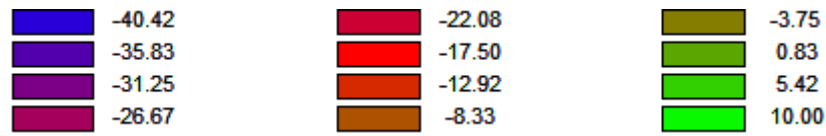


Figure 5.3: (a) vertical stress in specimen with plate connector and (b) vertical stress in specimen with shear studs

**Reinforcement stress: (MPa)**

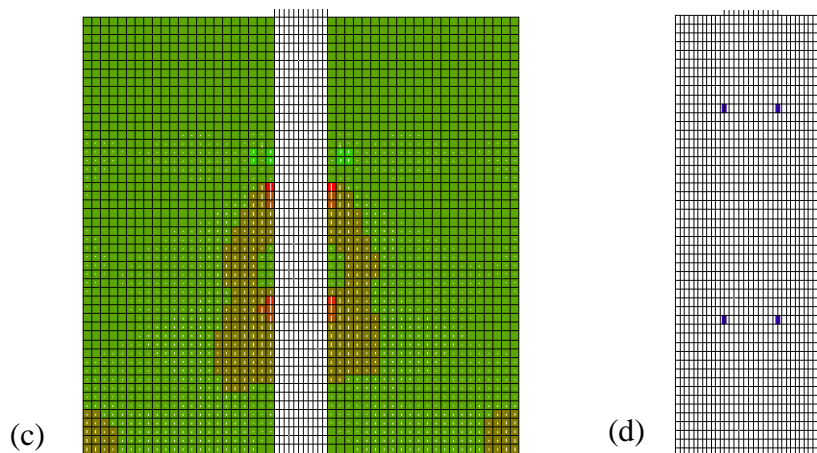
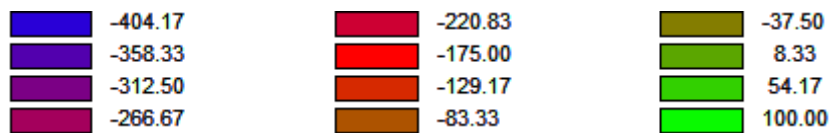


Figure 5.3: (c) stress in specimen with plate connector (d) stress in reinforcement used instead of studs

In this case the failure load is 1295kN which little bit higher then the steel profile capacity but much higher than our expected value. In specimen with plate connector, the stress in reinforcement is far below the yield stress so failure is in concrete. Moreover this is an idea only as the modeling is done with 2D program.

#### **5.4 Effect of concrete grade:**

This study mainly based on the mechanism of load transfer between steel and concrete interface where properties of concrete is really an important factor. To see the effect here all the analysis done with the Grade55 concrete and compare with Grade40 concrete.

Specimen	Theoretical design (kN)	With 40MPa concrete (kN)	With 55MPa concrete (kN)	% of change (+ve)
SP1A	965	970	970	0
SP1C	965	970	970	0
SPBM1	897	1027	1079.6	5.1
SPBM2	897	550	600	9.1
SPDM1	897	1629	1706.7	4.8
SPDM2	897	1500	1598	6.6
SPEM1	707	1295	1357.2	4.9

Table 5.4 Effect of concrete grade

Here in case of SP1A and SP1C the failure is occurring in shear stud so the failure load does not change with the concrete grade. In remaining cases the change is maximum in SPBM2 where plates are explicitly modeled and load is transferred to the concrete from both plate and web. And change is minimum in the specimen SPDM1 and SPEM1 where the specimens are modeled by connecting the element below the connector by perfect bonding at a certain interval where load is transferred only from web.

In general, from the result it can be said that if the concrete grade is change from 40 to 55 then there is around 6-7% increase in the total restrain force.

Details of the results are given in Annex A5.

## CHAPTER: SIX

### CONCLUSION

#### **6.1 Summary and conclusion:**

In this study, theoretical design and numerical analysis of some composite reinforced concrete specimens having different types of structural configuration is presented. The load transfer mechanism in each types of configuration is different. The results obtained from this study is summarized in the following table.

Specimen	SP1A	SP1C	SPBM1	SPBM2	SPDM1	SPDM2	SPEM2
Design load (kN)	965	965	897	897	897	897	770
FEM load (kN)	970	970	1027	550	1629	1500	1295

On the basis of the results and interpretation, following conclusion can be drawn:

1. To increase the shear resistance connectors are added so that it can act together with the bond and friction resistance between the steel profile and concrete. In this case flexible connectors like shear studs can be used to ensure that failure is occurring in the connection. In this study it shows that, in those specimens having only stud connector, the failure occurs in the studs when the stress in the concrete is far below its capacity. The reason is that this type of connector dose not exhibits similar load-slip relationship like steel profile and concrete which is really important in load transfer mechanism.
2. In case of rigid connectors like welded plate, it creates a strut and tie effect together with the tie bar which is a great advantage in load transfer. This study shows in FEM analysis, most of the case exhibit more restraining capacity then what expected. The failure occurs in concrete as the stress in reinforcement is considerably less than its capacity. Moreover most of the case it exceeded the theoretical capacity of plate itself, so there is a huge probability of failure occurring in the connection by plate itself specially in configuration D.
3. If both flexible and rigid types of connector are used, this study explained that the stud connectors cannot actually take part in load transfer mechanism that much, as most of the load transferred through plate connector. The reason is also same that both type of connector doesn't show similar load-slip characteristics.
4. All these cases in this study are involve with the theoretical design with existing design code and finite element analysis where a lots of facts are compromised. So conclusion can be drawn that, to get the real behavior of load transfer and clarify all those issues can be achieved by physical experiments.

## **6.2 Suggestion for future work:**

The present study covers only the design and numerical modeling but to get overall behavior of load transfer mechanism of hybrid structure, extensive and more details studies are required.

Some aspects are listed below as scope of future work in this area:

1. The investigation can be carried out in big range for experimental work in the laboratory to get the actual behavior and compare with the obtained result in this study.
2. In this study, most of the cases the failure load for the specimen is more than the steel profile capacity if S355 grade steel is used. So it suggested that instead of S355 higher grade steel should use.
3. An extensive parametric study can be done having different concrete grade, steel profile, connector types, configuring and reinforcement.
4. It is clear from the study that the load transfer mechanism is directly related with the area of concrete where the load is transmitted, so there can be an investigation about the effective width and thickness of the concrete zone.
5. In this study while modeling a lot of facts are compromise like reinforcement are consider as smeared instead of discrete, so further study can by performing more accurate modeling to get more accurate result and conclusion.

## **BIBLIOGRAPHY**

1. EC4 (2004). EN 1994-1-1 Eurocode 4- Design of composite steel and concrete structures- Part 1-1: General rules and rules for buildings.
2. Eurocode-2 (2004). Design of concrete structures-Part 1: General rules and rules for buildings. EN1992-1-1, European Committee for Standardization.
3. State of A on the identification of the fundamental force transfer mechanisms at steel-concrete interface. Smartcoco Project, 2013.
4. A. Plumier et al. Design for shear of columns with several encased steel profiles. A proposal. 2013.
5. C. Roeder et al., Shear connector requirements for embedded steel sections, *Journal of Structural Engineering*, 1999.
6. W. Xue, M. Dind et al., Static Behavior and Theoretical Model of Stud Shear Connectors, *Journal of Bridge Engineering*, 2008.
7. Li An & Krister Cederwall, Push-out Test on Studs in high strength and normal strength concrete, *J. Construct. Steel Res.* Vol. 36, No. 1, pp. 15-29, 1996.
8. Md. Khasro Miah, Strain Behavior of Shear Connectors in Composite Structures, *DUET Journal*, Vol. 1, Issue 1, June 2010.
9. H.B. Shim, Push-out tests on shear studs in high strength concrete, 2010 Korea Concrete Institute, Seoul, ISBN 978-89-5708-181-5.
10. Mohammad Makki Abbass, Performance Evaluation of Shear Stud Connectors in Composite Beams with Steel Plate and RCC slab, *International Journal of Earth Sciences and Engineering*, ISSN 0974-5904, Volume 04, No 06 SPL, October 2011.
11. Buttry, K. E. (1965). Behavior of stud shear connectors in lightweight and normal-weight concrete, Univ. of Missouri, Rolla, Mo. PhD.
12. Chapman, J. C. (1964). "Composite construction in steel and concrete - The behaviour of composite beams." *The Structural Engineer* 42(4): 115-125.
13. Corley, G. W. & Hawkins, N. M. (1968b), 'Shearhead reinforcement for slabs', *Journal of the American Concrete Institute* 65, 811-824.
14. Hanswille, G. (2002). Push Out Tests with Groups of Studs, ECSC Steel RTD Programme: Composite Bridge Design for Small and Medium Spans. Final report 7210-PR/113, Ch. 3, pp. 3-1, 3-43.
15. Hosaka, T., et al. (1998). "An experimental Study on Characteristics of Shear Connectors in Composite Continuous Girders for Railway Bridges (in Japanese)." *Journal of structural Engineering*, JSCE 44A: 1497-1504.
16. Boyan Mihaylov (2008), Behaviour of Deep Reinforced Concrete Beams under Monotonic and Reversed Cyclic Load, Ph.D. thesis.

# ANNEX

## A SP1.

### **Reinforcements:**

Design requirements [EC 2.1.- §1 9.6]:

- the area of vertical reinforcement should lie between  $A_{s,vmin} = 0.002 \cdot A_c$  and  $A_{s,vmax} = 0.04 \cdot A_c$  ;
- the distance between two vertical bars should not exceed 3 times the wall thickness or 400 mm;
- the area of horizontal reinforcement should not be less than  $A_{s,hmin} = 0.001 \cdot A_c$  ;
- the distance between two horizontal bars should not be more than 400 mm;

### **Strut and Tie model:**

Case A – The horizontal reinforcement is determined according to Figure 3 – case A. The concrete compression struts are formed assuming an angle  $\alpha = 45^\circ$ . The tie force T presented

in Figure 3 is expressed with the following formula:  $T = \frac{P_{Rk}}{2} = 40.21\text{kN}$

The link area needed to be placed under one shear stud is:  $A_{link} = \frac{T}{f_{sd}} = 0.81\text{cm}^2$

$1\Phi 12 = 1.13\text{ cm}^2 > A_{link}$ . 1  $\Phi 12$  link rebar will be placed at distance of  $s_c = 150\text{mm}$ ;

$\frac{H}{s_c} = \frac{1000\text{mm}}{150\text{mm}} \approx 7$  link rebars on one side of the concrete wall.

Vertical reinforcement is considered as 6  $\Phi 10$  on one side of the concrete wall. The total amount of vertical reinforcement is  $A_{sl} = 2 \cdot A_{\phi 10} = 9.42\text{cm}^2$  placed at a distance of 185 mm.

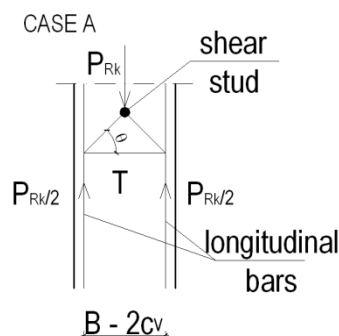


Figure . Case A – Strut and Tie model.

Case C -According to Figure 4:  $T = \frac{P_{Rk}}{2} = 40.21$ . The horizontal amount of reinforcement is:

$A_{sh} = \frac{T}{f_{sd}} = 0.81\text{cm}^2$ . 1  $\Phi 12$  reinforcement bar at distance of  $s_c = 150\text{ mm}$  will be placed.



$\frac{H}{s_c} = 1000\text{mm} / 150\text{mm} \approx 7$  rebars on one side of the concrete wall, as indicated in Figure

2C; total amount of horizontal area is:  $A_{sh} = 2 \cdot A_{7\phi 12} = 15.82\text{cm}^2$ . Vertical reinforcement is the same as in configuration A.

#### A SP2:

#### **Strut and tie model for horizontal reinforcement**

The concrete compression struts are formed assuming an angle  $\alpha = 45^\circ$ , as shown in Figure 6.

The tie force is equal to:  $F_{tie} = V_{Rd,1plate} = 112.12\text{kN}$ .

The horizontal hoops placed on a distance equal to  $s_p = 250\text{mm}$  is:

$$A_{hoop} = \frac{F_{tie}}{f_{sd}} = 2.24\text{cm}^2$$

$$2\Phi 12 = 2.26 \text{ cm}^2 > A_{hoop}$$

Case b2): 1  $\Phi 12$  horizontal hoop will be placed at a distance of  $s_p/2 = 125 \text{ mm}$ .

Case b3): 2  $\Phi 12$  horizontal ties will be placed at a distance of  $s_p = 250 \text{ mm}$ .

EC 2.1. –§8.4.3(2) The basic required anchorage length  $l_{b,rqd}$  is:

$$l_{b,rqd} = \frac{\phi}{4} \cdot \frac{\sigma_{sd}}{f_{bd}} = 12\text{mm} / 4 \cdot 500\text{MPa} / 2.5\text{MPa} = 300\text{mm}$$

where:

$$f_{bd} = 2.25 \cdot \eta_1 \cdot \eta_2 \cdot f_{ctd} = 5.63\text{MPa}$$

$\eta_1 = 1$  coefficient related to the quality of the bond condition;

$\eta_2 = 1$  for  $\Phi < 32 \text{ mm}$ ;

$$f_{ctd} = \frac{\alpha_{ctd} \cdot f_{ctk,0.05}}{\gamma_c} = 1 \cdot 2.5\text{MPa} / 1 = 2.5\text{MPa} \text{ the value of design tensile strength;}$$

$\sigma_{sd} = 500\text{MPa}$  of design stress of the bar;

Case d2): 1  $\Phi 12$  horizontal hoops will be placed at a distance of  $s_p/2 = 125 \text{ mm}$ .

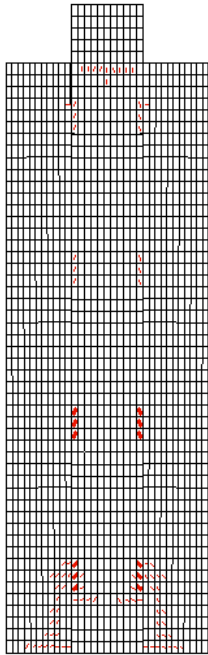
where:

$s_p = 250 \text{ mm}$  is the distance between 2 plate connectors.

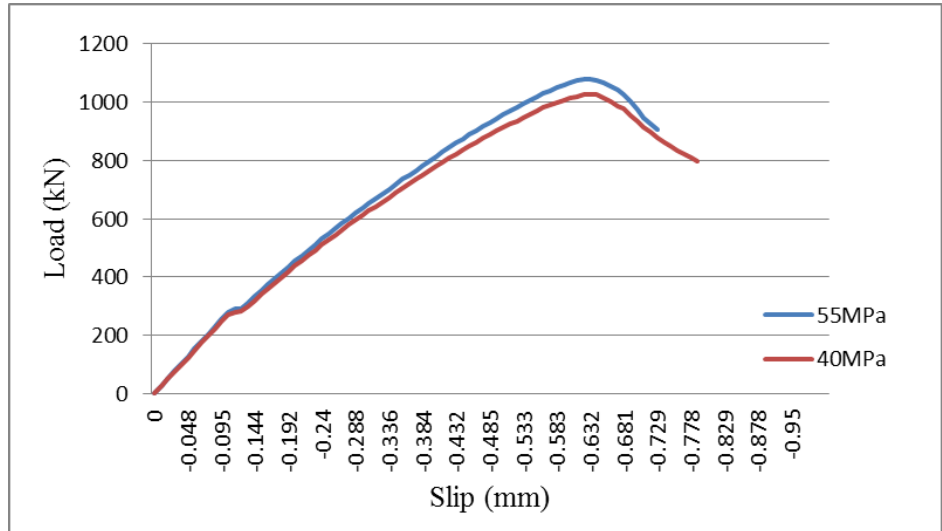
Vertical reinforcement is considered as 6  $\Phi 10$  on one side of the concrete wall. The total amount of vertical reinforcement is  $A_{sl} = 2 \cdot A_{6\phi 10} = 9.42\text{cm}^2$  placed a distance of 185 mm.

A5:

### 1. SPBM1:

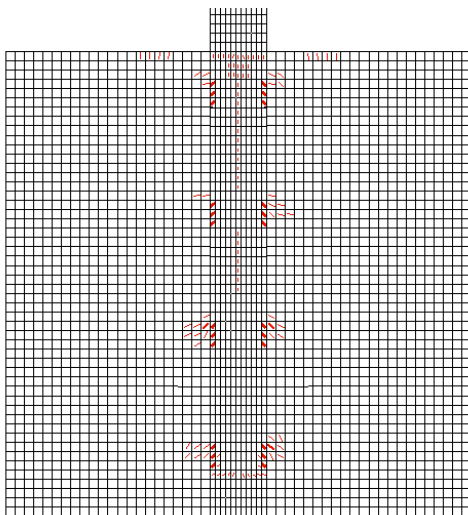


Cracked View

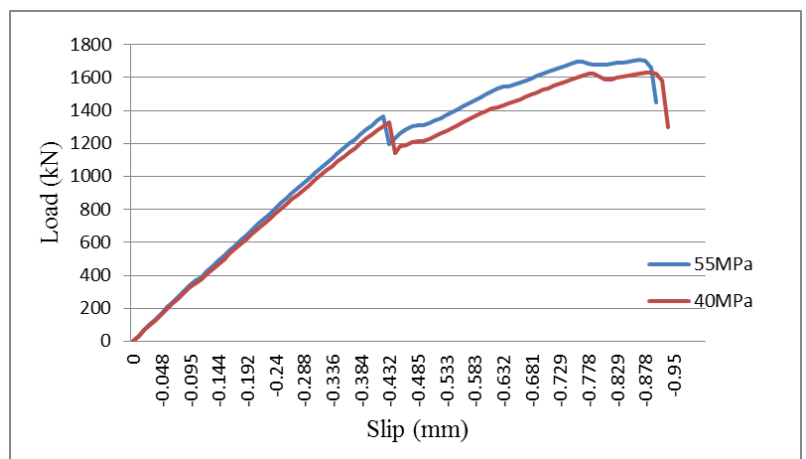


Load-Slip curve for SPBM1

### 2. SPDM1:

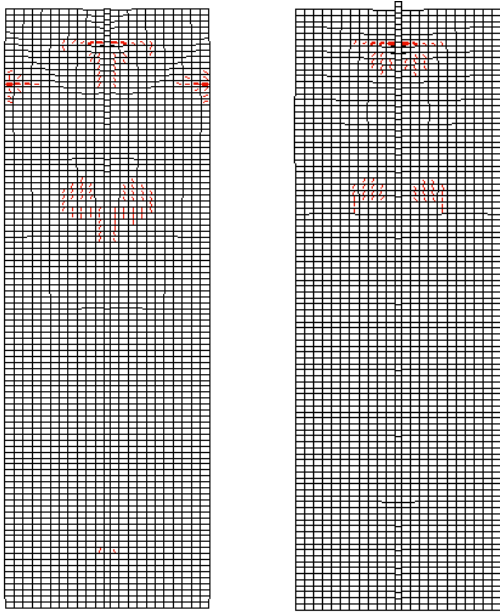


Cracked View

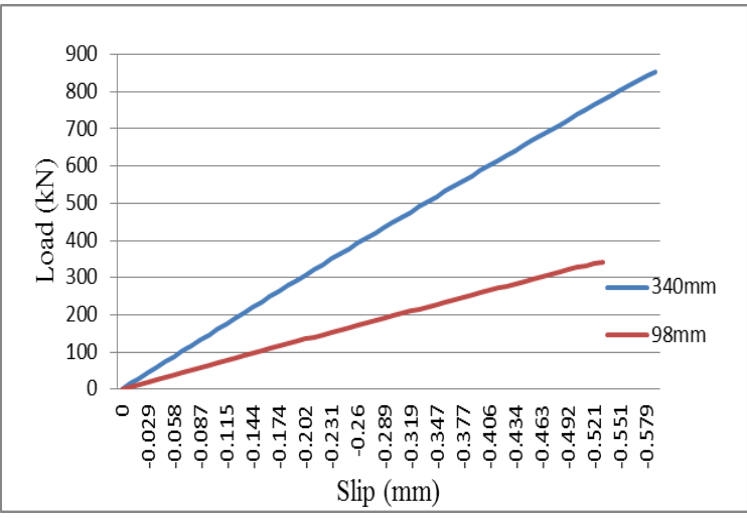


Load-Slip curve for SPDM1

### 3. SPBM2:

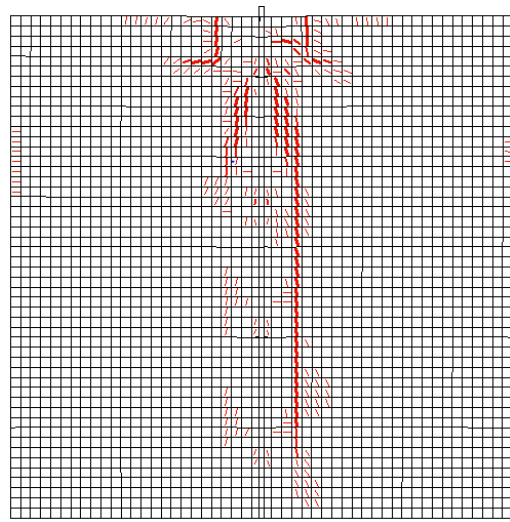
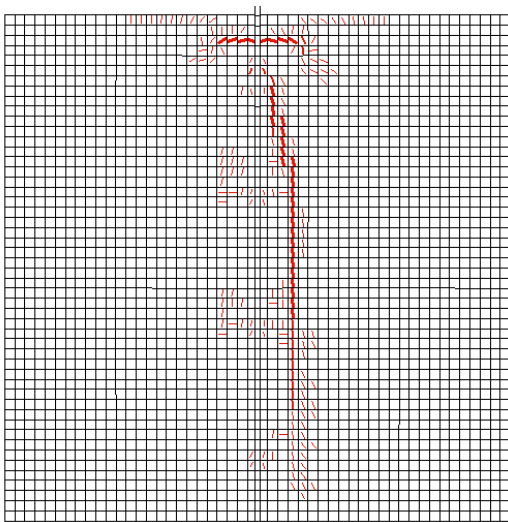


Cracked View 340mm and 98 mm

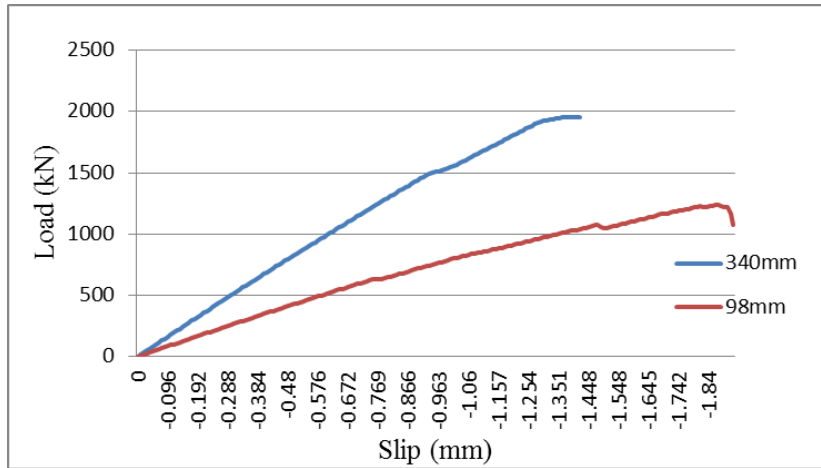


Load-Slip curve for SPBM2

### 4. SPDM2:

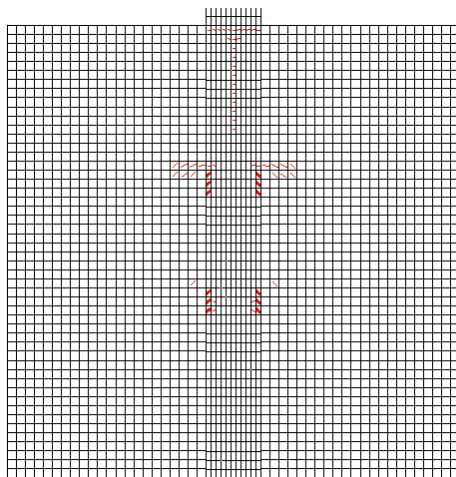


Cracked View 340mm and 98 mm

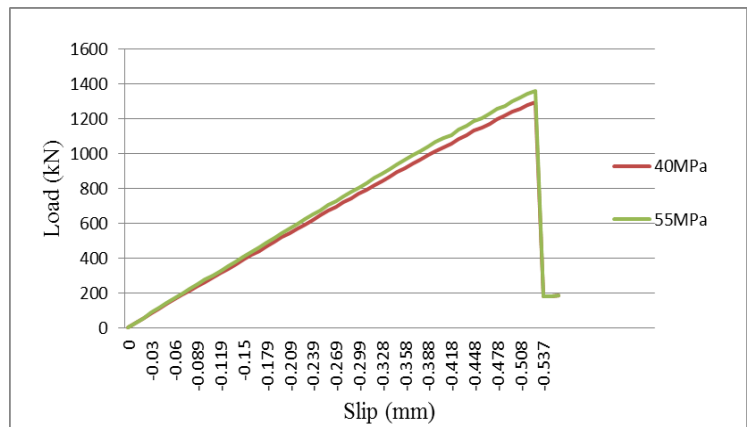


Load-Slip curve for SPDM2

5. SPEM1:



Cracked View



Load-Slip curve for SPEM1

-----